

Extended iterative scheme for QCD: the four-gluon vertex

L. Driesen, M. Stingl

Institute for Theoretical Physics I, University of Münster, D-48149 Münster (Westf.), Germany

Received: 1 September 1998 / Revised version: 23 December 1998

Communicated by F. Lenz

Abstract. We study the self-consistency problem of the generalized Feynman rule (nonperturbatively modified vertex of zeroth perturbative order) for the 4-gluon vertex function in the framework of an extended perturbation scheme accounting for non-analytic coupling dependence through the Λ scale. Tensorial structure is restricted to a minimal dynamically closed basis set. The self-consistency conditions are obtained at one loop, in Landau gauge, and at the lowest approximation level ($r = 1$) of interest for QCD. At this level, they are found to be linear in the nonperturbative 4-gluon coefficients, but strongly overdetermined due to the lack of manifest Bose symmetry in the relevant Dyson-Schwinger equation. The observed near decoupling from the 2-and-3-point conditions permits least-squares quasisolutions for given 2-and-3-point input within an effective one-parameter freedom. We present such solutions for $N_F = 2$ massless quarks and for the pure gluon theory, adapted to the 2-and-3-point coefficients determined previously.

1 The generalized Feynman rule $\Gamma_{4V}^{[r,0]}$

The present paper continues, and brings to a provisional stage of completion, the determination of generalized Feynman rules in an extended perturbation scheme for QCD [1], designed to account for the strongly nonanalytic coupling dependence of correlation functions through the renormalization-group invariant mass scale Λ . The generalized rules, denoted $\Gamma^{[r,0]}$, are proper vertex functions of zeroth perturbative order (no power corrections in the coupling g^2 , as indicated by the index 0), but with a nonperturbative Λ dependence which in turn is approximated systematically at a level characterized by the index r . In contrast to the ordinary Feynman rules, it is a nontrivial self-consistency problem for these extended rules to reproduce themselves in the integral equations for vertex functions. However, the divergence-related mechanism operative in the self-reproduction [1] does ensure that formation of $\Gamma^{[r,0]}$'s remains rigorously restricted to the small number of vertices corresponding to the ordinary Feynman rules – the superficially divergent vertices. In the companion paper [2], this self-consistency problem was set up and solved for the vertices with up to three external legs, on the lowest nontrivial approximation level ($r = 1$, and one loop) of interest for QCD.

Below, we complement this study by examining the highest superficially divergent amplitude, the 4-vector (4-gluon) vertex Γ_{4V} [3]. There are several features that set this vertex function apart and motivate its separate treatment. One is its sheer kinematical complication, due partly to the large number of 6 Lorentz-scalar momen-

tum variables, but mostly to the exorbitantly lengthy tensor decompositions implied by its 4 color and 4 Lorentz indices. In constructing the $r = 1$ approximant $\Gamma_{4V}^{[r,0]}$ (Sect. 2), one is thereby forced to adopt a theoretically motivated simplification of the full tensor structure. Another special feature is that Γ_{4V} represents the lowest QCD amplitude which in the nonperturbative context exhibits the phenomenon of *compensating poles* (or, in the terminology of [2], of negative *shadow poles*), first noted in Abelian models in [4]. While these poles can be inferred uniquely already from the “lower” DS equations for Γ_{3V} and Γ_{2V} by suitable residue-taking operations, it is now necessary to demonstrate that on the level of the 4-point equation they are in turn self-consistent (Sect. 3). A natural by-product of this demonstration is then a “reduced” integral equation for the remainder vertex V_{4V} defined by

$$\Gamma_{4V}^{[r,0]} = -(C_1^{[r]})_{2V,2V} - (C_2^{[r]})_{2V,2V} - (C_3^{[r]})_{2V,2V} + V_{4V}^{[r,0]}, \quad (1.1)$$

where $C_{1,2,3}^{[r]}$ are the shadow-pole terms in the 3 channels of the 4-gluon amplitude. This amounts to rearranging the full connected-and-amputated 4-gluon correlation function as

$$T_{4V} = A'_1 + A'_2 + A'_3 + V_{4V}, \quad (1.2)$$

where $A'_{1,2,3}$ are “softened”, i.e. one-shadow-irreducible, one-gluon exchange diagrams formed by subtracting the shadow-pole term from the ordinary dressed-one-gluon-exchange diagram $A_{1,2,3}$ in each of the 3 channels. The

object $V_{4V}^{[r;0]}$ depends on only four Lorentz- scalar variables, and establishing the self-consistency conditions for its nonperturbative coefficients (Sect. 4) is simpler than for the full Γ_{4V} .

The latter conditions will exhibit a problem that presumably besets all approximate treatments of vertex equations with three or more external lines: if such vertices possess a symmetry among their external legs such as Bose symmetry, their Dyson-Schwinger (DS) equations will in general not display this symmetry manifestly, and any approximation to them will produce unsymmetric terms. Forcing self-reproduction of a symmetric input by requiring these terms to vanish leads to *overdetermination* of the dynamical conditions. If this does not happen to be counteracted by underdetermination tendencies, as was the case for the $r = 1$ three-point conditions derived in [2], one must settle for a “compromise” solution in the sense of least-squares error minimization (Sect. 5).

Technically, the self-consistency conditions will be derived at the $r = 1$ and one-loop ($l = 1$) levels, and in *Landau gauge*. The latter again provides considerable simplification because with this gauge fixing the two ghost vertices *at one loop* remain perturbative, and because a closed DS system can be written for the amplitudes with only transverse (if any) gluon legs, whose tensorial complexity is significantly lower. A disadvantage, of course, is that the self-consistency (or lack of it) for statements concerning longitudinal-gluon amplitudes, such as Slavnov-Taylor (ST) identities at finite momenta, cannot be checked directly from such a system. *Differential* four-gluon ST identities with one momentum vanishing, which to our knowledge have not been studied so far, would, in analogy to the 3-gluon case, constrain also the fully transverse vertex if one imposes certain regularity assumptions in addition to BRS invariance. In the present paper we do not consider these identities; since their kinematical complexity is of the same order as for the vertex itself, they represent a large problem in themselves that must form a subject of future study.

The 4-gluon vertex also occupies a special position in that it belongs both to the class of superficially divergent “basic” vertices having their own (ordinary or extended) Feynman rules, and to the class of amplitudes capable of developing bound-state (here, glueball) poles – a phenomenon otherwise restricted to the superficially *convergent* higher vertices. In the present paper we are exclusively concerned with the generalized Feynman rule, a *zeroth-order* quantity, which like its ordinary counterpart contains no information as yet about bound states. The latter, if present, arise from an infinite partial resummation of the *higher-order*, quasi-perturbative corrections

$$[g(\nu)^2]^p \cdot \Gamma_{4V}^{[r;p]}(\{k\}, A, \nu) \quad (p = 1, 2, 3, \dots). \quad (1.3)$$

As the notation recalls, these have their own nonperturbative Λ dependences, which may be complemented by an inversely logarithmic “perturbative” dependence when reparametrizing the quasi-perturbative series in terms of $\alpha_s(k^2)$ rather than $g^2(\nu)$. Upon ladder or similar resummation, these may build up a pole in some Mandelstam

variable (the squared sum of some subset of the momenta $\{k\}$) at some multiple of Λ^2 representing the square of a bound-state mass. Such a pole is accompanied by a pair of residue functions, each representing an infinite power series in g^2 starting at least with $p = 1$. It is therefore an example of nonperturbative Λ dependence embedded in an otherwise quasi-perturbative term (starting at least at order $p = 2$) of the amplitude. These characteristics should prevent confusion between bound-state poles and the poles which in the present scheme arise *as rational approximations to branch cuts* in the squares of single-external-line momenta, and *in zeroth quasi-perturbative order*. The 4-gluon function is unique in exhibiting both phenomena. It is yet another matter (and not touched upon in this article) that in a confining theory the calculation of *S-matrix elements* will require a still larger set of generalized Feynman rules, comprising hadron-to-quarks and hadron-to-gluons bound-state vertices for the outer corners of S-matrix diagrams – vertices of an intrinsically hybrid nature, since their dependence on the squares of single-quark momenta would have to be determined and approximated consistently with the generalized Feynman rules for the internal lines and vertices, whereas their dependence on the total virtuality of the bound state is governed by “resummed-perturbative” bound-state dynamics.

2 Structure of the $r = 1$ approximant

Due to the large number of possible tensor structures of a four-gluon amplitude (e.g., 43 independent Lorentz tensors for a fully transverse amplitude, each combined with 8 independent color tensors for $SU(3)_C$), one is forced, at the present stage, to adopt some theoretically motivated restriction to a smaller subset of tensors. We briefly describe such a restricted form, partly repeating material from Appendix A of [1] to keep the discussion self-contained. The amplitude

$$\left(V_{4V}^{[r;0]}(p_1, p_2, p_3, p_4) \right)_{abcd}^{\kappa\lambda\mu\nu} \quad (p_1 + p_2 + p_3 + p_4 = 0) \quad (2.1)$$

is expanded over an 18-member set of color \otimes Lorentz tensors, of which 15 are linearly independent. They are formed from building blocks

$$C_{abcd}^{(i)} L_{(j)}^{\kappa\lambda\mu\nu} \quad (i = 1 \dots 6, j = 1 \dots 3), \quad (2.2)$$

where the color tensors $C^{(i)}$, fourth-rank objects over the adjoint representation of $SU(3)_C$, are given by

$$\begin{aligned} C_{abcd}^{(1)} &= \delta_{ab} \delta_{cd}, & C_{abcd}^{(2)} &= \delta_{ac} \delta_{db}, \\ C_{abcd}^{(3)} &= \delta_{ad} \delta_{bc}, \end{aligned} \quad (2.3)$$

$$\begin{aligned} C_{abcd}^{(4)} &= f_{abn} f_{cdn}, & C_{abcd}^{(5)} &= f_{acn} f_{dbn}, \\ C_{abcd}^{(6)} &= f_{adn} f_{bcn}, \end{aligned} \quad (2.4)$$

in terms of the $SU(3)$ structure constants f_{abc} . Only five of these are linearly independent, since $C^{(4)} + C^{(5)} + C^{(6)} = 0$

by the Jacobi identity. As compared to the most general structure, this set omits three tensors containing a symmetric $SU(3)$ structure constant d_{abc} . The Lorentz-tensor building blocks $L_{(j)}$ are the three dimensionless ones,

$$\begin{aligned} L_{(1)}^{\kappa\lambda\mu\nu} &= \delta^{\kappa\lambda}\delta^{\mu\nu}, & L_{(2)}^{\kappa\lambda\mu\nu} &= \delta^{\kappa\mu}\delta^{\nu\lambda}, \\ L_{(3)}^{\kappa\lambda\mu\nu} &= \delta^{\kappa\nu}\delta^{\lambda\mu}, \end{aligned} \quad (2.5)$$

which are linearly independent. In obvious ways, all these fall into crossing triplets, where second and third members in each triplet arise from the first member by the crossing operations,

$$\text{“} s \rightarrow u \text{“} \quad : \quad (2, 3, 4) \rightarrow (3, 4, 2), \quad (2.6)$$

$$\text{“} s \rightarrow t \text{“} \quad : \quad (2, 3, 4) \rightarrow (4, 2, 3), \quad (2.7)$$

the s channel being by convention the $(1+2) \leftrightarrow (3+4)$ channel. Here 2 stands for the set (p_2, λ, b) , etc.

The set (2.2–2.5) is distinguished in that it constitutes the *smallest dynamically closed subset* of the full tensor structure, i.e.:

(i) It closes under Bethe-Salpeter (BS) iteration in each of the three channels of the amplitude, as exemplified by the s -channel, color-space multiplication,

$$\left(C^{(i)} \cdot C^{(j)} \right)_{abcd} = \sum_{e,f=1}^8 C_{abe f}^{(i)} C_{efcd}^{(j)}, \quad (2.8)$$

and closes also under iteration of DS interaction diagrams, provided the 3-gluon vertices involved have f_{abc} color structure only. We emphasized earlier [2] that with 4-gluon color dependence restricted to the five-dimensional basis (2.3/2.4), it would be inconsistent to retain d_{abc} color structure in the 3-gluon vertex, since the tensors omitted on the 4-gluon level would also contribute to that structure via the hierarchical coupling in the 3-gluon DS equation.

(ii) It closes under the crossing operations connecting the three channels, as given by (2.6) and (2.7).

(iii) It contains the perturbative zeroth-order vertex, namely,

$$\begin{aligned} \Gamma_{4V}^{(0)pert} &= \frac{3}{2} C^{(4)} (L_{(2)} - L_{(3)}) \\ &+ \frac{1}{2} \left(C^{(5)} - C^{(6)} \right) (-2L_{(1)} + L_{(2)} + L_{(3)}). \end{aligned} \quad (2.9)$$

(Without this property, there would exist a still smaller dynamically closed set comprising only the tensors (2.3), but maintaining the perturbative limit calls for inclusion of (2.4)). All these statements are easy to verify by direct calculation.

While this closedness property represents the primary motivation for the use of the dynamically minimal tensor basis, additional motivation for the choice (2.5) of Lorentz tensors comes from the observation that these are the only ones accompanied by invariant functions of zero mass dimension. The tensors omitted in (2.5) contain two or four powers of momentum, and are thus associated with invariant functions of mass dimensions -2 or -4 . Since our

approximants contain the dimensionful Λ scale, this does not yet imply that loop integrals contributing to these functions must all be convergent, but inspection shows that possibilities for the formation of such tensor structures are nevertheless strongly restricted. First, the requirement of asymptotic freedom despite the presence of positive momentum powers in the tensor, together with the fact that zeroth-order forms must have at least one power of Λ^2 in each term, leaves few allowed terms in the first place for approximants to such invariant functions. Second, for each particular allowed term, possibilities for it to emerge with a divergent-integral factor from the r.h.s. of the relevant DS equation, as necessary for zeroth-order self-reproduction, turn out to be very limited if existent at all. As an example, consider a term of type

$$[\delta^{\kappa\lambda} p_4^\mu p_3^\nu] \times \frac{\Lambda^2}{(p_3^2 + u_2 \Lambda^2)(p_4^2 + u_2 \Lambda^2)}, \quad (2.10)$$

which may be present in the fully transverse V_{4T} and is allowed by its large-momentum behavior. It is straightforward to check that in the integral equation (Fig. 10 below) we are going to use for V_{4T} , the DS terms with only three-point vertices – diagrams $(A2)_4$, $(C1)_4$, $(E1)_4$, $(E1')_4$ – cannot produce a zeroth-order term of this form: the two denominator factors of (2.10) can come only from two *different* three-point vertices, but then each of them will bring at least one Λ^2 factor, and the remaining, dimensionless loop integral cannot factor out the two numerator momentum components without becoming convergent. On the other hand the DS diagrams where V_{4V} itself enters – diagrams $(A3)_4$, $(C2)_4$ and the E element of diagram $(A1)_4$ in Fig. 10 – can produce such a term but only, by the same logic, where it is already pre-existent as part of a $V4$ term and can factor out as a whole while leaving a logarithmically divergent integral. It is easy to check that this leaves only the possibilities for the above term (i) to “feed on itself” or (ii) to feed on terms of the more complicated form

$$[p_2^\kappa p_1^\lambda p_4^\mu p_3^\nu] \times \frac{\Lambda^2}{(p_{1or2}^2 + u_2 \Lambda^2)(p_3^2 + u_2 \Lambda^2)(p_4^2 + u_2 \Lambda^2)}, \quad (2.11)$$

with a dimension-4 tensor. Such terms, in turn, have still more restricted possibilities for self-reproduction in that they can only “feed on themselves” through the E element of term $(A1)_4$. But on the one-loop level, where the curly bracket of $(A1)_4$ does not yet depend on four-gluon coefficients, this means that the equation for the coefficient of (2.11) is linear and homogeneous, and generically (i. e. except for improbable special configurations of 2- and 3-point coefficients) permits only the trivial, zero solution. Then, however, the equation for the coefficient of (2.10) also becomes linear and homogeneous, and one concludes that on the one-loop level of the self-consistency problem, these two types of terms do not reproduce in zeroth order. Without going through the large number of other special cases, we remark that in view of such restrictions it makes sense, as a first step, to stay with the dimensionless Lorentz tensors (2.5), at least to one-loop order.

Invariant functions for the V_{4V} amplitude, we recall, have *zeroth-order* rational structure only with respect to the variables $p_1^2 \dots p_4^2$, since the entire zeroth-order rational structure with respect to s, u, t variables is borne by the compensating-pole terms of (1.1). Since our earlier demonstration of this applies, strictly speaking, only to the color-octet channels, we check in Appendix A of this paper that in fact it holds generally. Thus at order $r = 1$, all invariant functions involve the same, fully symmetric denominator

$$\Delta^{[1,0]} = (p_1^2 + u_2'' \Lambda^2) (p_2^2 + u_2'' \Lambda^2) \times (p_3^2 + u_2'' \Lambda^2) (p_4^2 + u_2'' \Lambda^2). \quad (2.12)$$

Numerator polynomials in Λ^2 and the squared momenta, of mass dimension 8, must conform to the restrictions of naive asymptotic freedom. As seen in [2] in the example of the 3-gluon vertex, additional restrictions arise from the requirement that “softened” (one-shadow-irreducible) one-gluon exchange diagrams, which represent the *physical* one-gluon exchange mechanism, again should not generate higher-than-perturbative degrees of divergence when inserted in loops (for an example, see the right-hand portion of diagram $(A3)_4$ in Fig. 10): this excludes terms in the rational approximant in which any one squared momentum has a net positive power. Thus numerator polynomials should not contain s, t, u either, nor should they have terms of type $\Lambda^2 p_i^6$ or $\Lambda^4 p_i^4$ still allowed by the primary restrictions. At level $r = 1$, all zeroth-order rational structure can then be expressed in terms of the single-pole quantities

$$\Pi_i = \frac{\Lambda^2}{p_i^2 + u_2'' \Lambda^2} \quad (i = 1, 2, 3, 4), \quad (2.13)$$

and the general $r = 1$ approximant becomes a sum of terms, each featuring a product of a tensor of type (2.2) and of an invariant function built from the quantities (2.13).

With full Bose symmetry among the four legs imposed, this approximant turns out to involve seventeen dimensionless, real coefficients. There are several ways of arriving at this number, but the first step is always to realize that each of the color tensors (2.3/2.4) and Lorentz tensors (2.5) brings a definite *partial permutation symmetry within one channel*, and thereby imposes a corresponding partial symmetry on its accompanying factors. Consider e.g. the s channel, and denote by the symbol

$$\{\pi_{12}, \pi_{34}; \pi_s\} \quad (\text{each } \pi = +1 \text{ or } -1) \quad (2.14)$$

the class of four-point amplitudes having parities $\pi_{12}, \pi_{34}, \pi_s$ under the $1 \leftrightarrow 2, 3 \leftrightarrow 4$, and $(1, 2) \leftrightarrow (3, 4)$ permutations respectively. Then the color tensor $C^{(1)}$ of (2.3) has $\{+, +; +\}$ symmetry. The accompanying Lorentz tensors (2.5) can, with regard to this channel, be classified into $L_{(1)}$ and $L_{(2)} + L_{(3)}$, which are in class $\{+, +; +\}$, and $L_{(2)} - L_{(3)}$, which belongs to class $\{-, -; +\}$ (it is part of the special simplicity of the dynamically minimal basis that it contains no tensors with $\pi_s = -$). Then the way

the $C^{(1)}$ tensor can appear in the approximant is uniquely fixed to read,

$$C^{(1)}[L_{(1)}S + (L_{(2)} + L_{(3)})S' + (L_{(2)} - L_{(3)})A''], \quad (2.15)$$

where S, S' are invariant functions, built from the elements (2.13), in class $\{+, +; +\}$, and A'' is a function in class $\{-, -; +\}$. Full Bose symmetry then requires adding to (2.15) its inter-channel permutations (2.6) and (2.7); this also fixes uniquely the occurrence of the color tensors $C^{(2)}, C^{(3)}$. In an analogous way, the appearance of the tensor $C^{(4)}$ of (2.4) is fixed uniquely as

$$C^{(4)}[L_{(1)}A + (L_{(2)} + L_{(3)})A' + (L_{(2)} - L_{(3)})S''], \quad (2.16)$$

where A, A' are invariant functions in $\{-, -; +\}$ and S'' is in class $\{+, +; +\}$. Ignoring at first the linear dependence in (2.4), full symmetrization is again achieved by adding the permutations (2.6) and (2.7) with $C^{(5)}, C^{(6)}$ color tensors. Now for each S -type invariant function there are, at $r = 1$, five possible building blocks, namely, in the notation of (B.1) to (B.4) of Appendix B.1, the quantities $G_{(1)}, G_{(2s)}, G_{(2u)} + G_{(2t)}, G_{(3)}, G_{(4)}$, whereas for the A -type functions only one building block, namely $G_{(2u)} - G_{(2t)}$, is available. Thus for the moment we have $3 \times 5 + 3 \times 1 = 18$ coefficients. To account for the linear dependence of the tensors (2.4) one eliminates, for example, $C^{(5)} + C^{(6)}$ in favor of $-C^{(4)}$, then alternatively $C^{(6)} + C^{(4)}$ in favor of $-C^{(5)}$; the two expressions, apart from a permutation (2.6) of momenta, must display the same coefficients. This turns out to impose one relation between the coefficients of A, A', S'' ; the two other ways of conducting the eliminations produce the same relation. As stated, one ends up with 17 independent coefficients.

In the following we use two different representations for $V_{4V}^{[1,0]}$. The first can be viewed as a straightforward re-grouping of the form arising from the enumeration just described, and has building blocks with manifest Bose symmetry but involving linearly dependent color tensors internally; it uses and for our purpose defines the 17 independent coefficients. It is thus suitable for the *presentation* of the vertex as a generalized Feynman rule. This representation uses a color tensor

$$C_{abcd}^{(S)} = \text{tr}(t_a t_d t_b t_c) + \text{tr}(t_a t_c t_b t_d) \quad (2.17)$$

and its crossing partners $C^{(U)}, C^{(T)}$ obtained via (2.6) and (2.7), where t_n are the generator matrices of $SU(3)_C$ normalized by $\text{tr}(t_m t_n) = \frac{1}{2} \delta_{mn}$. The latter trace is then used to supply another tensor triplet, proportional to (2.3),

$$\text{tr}(t_a t_b) \text{tr}(t_c t_d) = \frac{1}{4} C_{abcd}^{(1)}, \quad (2.18)$$

plus crossing partners. $SU(3)$ representation algebra [6] gives the relation of (2.17) to (2.3/2.4) as

$$C^{(S)} = \frac{1}{12} [C^{(1)} + C^{(2)} + C^{(3)}] + \frac{1}{6} [C^{(5)} - C^{(6)}], \quad (2.19)$$

with analogous relations for $C^{(U)}, C^{(T)}$. In this basis, which has been used e.g. in work on the operator-product expansion [7], the vertex with four transverse gluon legs – the portion of V_{4V} which enters our purely transverse DS system based on Landau gauge fixing – is written

$$\begin{aligned} & \left[V_{4T}^{[1,0]}(p_1 \dots p_4) \right]_{abcd}^{\rho\sigma\tau\omega} = t^{\rho\kappa}(p_1) t^{\sigma\lambda}(p_2) t^{\tau\mu}(p_3) t^{\omega\nu}(p_4) \\ & \times \left\{ \left(\Gamma_{4V}^{(0)pert} \right)_{abcd}^{\kappa\lambda\mu\nu} + \sum_{n=1}^{17} \zeta_n \left(W_n^{[1,0]}(p_1^2 \dots p_4^2; \Lambda^2) \right)_{abcd}^{\kappa\lambda\mu\nu} \right\}, \end{aligned} \quad (2.20)$$

with the index T , as opposed to the generic V , now referring to transverse gluons, and with the t 's denoting transverse projectors in the external momenta. (Since our “minimal” tensor basis contains no tensors that would be removed completely by the transverse projections, the number of terms and coefficients in V_{4T} remains the same as in V_{4V} .) Each of the building blocks W_n comprises a color tensor (2.17) or (2.18) plus crossing partners, a combination of Lorentz tensors (2.5), and a combination of rational-function elements (2.13). Each therefore has at least one overall power of Λ^2 and vanishes in the perturbative limit, $\Lambda \rightarrow 0$. A full listing of these building blocks is relegated to Appendix B.1; here we write out just one of them for illustration:

$$\begin{aligned} & W_3^{[1,0]}(p_1^2 \dots p_4^2; \Lambda^2) = C^{(S)} (L_{(3)} - 2L_{(1)} + L_{(2)}) \\ & \times \left[\Pi_1 \Pi_4 + \Pi_2 \Pi_3 - 2(\Pi_1 \Pi_2 + \Pi_3 \Pi_4) + \Pi_1 \Pi_3 + \Pi_4 \Pi_2 \right] \\ & + C^{(U)} (L_{(1)} - 2L_{(2)} + L_{(3)}) \\ & \times \left[\Pi_1 \Pi_2 + \Pi_3 \Pi_4 - 2(\Pi_1 \Pi_3 + \Pi_4 \Pi_2) + \Pi_1 \Pi_4 + \Pi_2 \Pi_3 \right] \\ & + C^{(T)} (L_{(2)} - 2L_{(3)} + L_{(1)}) \\ & \times \left[\Pi_1 \Pi_3 + \Pi_4 \Pi_2 - 2(\Pi_1 \Pi_4 + \Pi_2 \Pi_3) + \Pi_1 \Pi_2 + \Pi_3 \Pi_4 \right] \end{aligned} \quad (2.21)$$

Note that these 17 building blocks are linearly independent of each other; the linear dependence of the basis tensors $C^{(S,U,T)}$ affects only their *internal* structure, which upon rewriting in terms of independent tensors would lose its manifest crossing (and therefore Bose) symmetry. However, as a representation of the *total* V_{4V} , (2.20) is based on dependent color tensors.

The second representation is more suitable for the self-consistency *calculation* of the zeroth-order vertex. To permit tensor-by-tensor comparison of the two sides of a DS equation, such a representation must employ linearly independent color tensors, and consequently forgo manifest Bose symmetry. However, since the way a $4V$ vertex appears in a DS interaction diagram singles out one of the three channels (compare, e.g., the $4V$ vertex in diagrams $(A3)_4$ or $(C2)_4$ of Fig. 10), it is useful to maintain partial symmetry properties within one channel. At first the *entire* vertex is classified in this way, without worrying about crossing. A basis of this kind, adapted to the s channel, has color tensors

$$C^{(A)} \equiv C^{(1)}, \quad C^{(B)} = C^{(2)} + C^{(3)},$$

$$C^{(E)} = C^{(5)} - C^{(6)}, \quad (2.22)$$

$$C^{(C)} = C^{(2)} - C^{(3)},$$

$$C^{(D)} \equiv C^{(4)} \left(= -C^{(5)} - C^{(6)} \right), \quad (2.23)$$

and Lorentz tensors (in $D = 4 - 2\epsilon$ Euclidean dimensions),

$$L_{(0)} = \frac{1}{D} L_{(1)}, \quad L_{(+)} = \frac{1}{2} (L_{(2)} + L_{(3)}) - \frac{1}{D} L_{(1)}, \quad (2.24)$$

$$L_{(-)} = \frac{1}{2} (L_{(2)} - L_{(3)}). \quad (2.25)$$

The latter have been chosen to display, under s -channel tensor multiplication, the projector-like properties,

$$L_{(m)}^{\kappa\lambda\rho\sigma} L_{(n)}^{\rho\sigma\mu\nu} = \delta_{mn} L_{(m)}^{\kappa\lambda\mu\nu} \quad (m, n = +, 0, -). \quad (2.26)$$

Among the fifteen product tensors $C^{(i)} L_{(j)}$ formed from (2.22/2.23) and (2.24/2.25) there are eight in class $\{+, +; +\}$ and seven in class $\{-, -; +\}$. In the decomposition

$$\begin{aligned} & \left(V_{4T}^{[1,0]}(p_1 \dots p_4) \right)_{abcd}^{\rho\sigma\tau\omega} = t^{\rho\kappa}(p_1) t^{\sigma\lambda}(p_2) t^{\tau\mu}(p_3) t^{\omega\nu}(p_4) \\ & \times \sum_{i=A\dots E} \sum_{j=+,0,-} C_{abcd}^{(i)} L_{(j)}^{\kappa\lambda\mu\nu} F_{i,j}^{[1,0]}(p_1^2 \dots p_4^2; \Lambda^2), \end{aligned} \quad (2.27)$$

the invariant functions $F_{i,j}$ therefore again come in two types,

$$\begin{aligned} & F_{(i,j) \in \{+, +; +\}}^{[1,0]} = \eta_{i,j,0} + \eta_{i,j,1} (\Pi_1 + \Pi_2 + \Pi_3 + \Pi_4) \\ & \quad + \eta_{i,j,2} (\Pi_1 + \Pi_2) (\Pi_3 + \Pi_4) \\ & \quad + \eta_{i,j,4} (\Pi_1 \Pi_2 + \Pi_3 \Pi_4) \\ & \quad + \eta_{i,j,5} [\Pi_1 \Pi_2 (\Pi_3 + \Pi_4) + (\Pi_1 + \Pi_2) \Pi_3 \Pi_4] \\ & \quad + \eta_{i,j,6} (\Pi_1 \Pi_2 \Pi_3 \Pi_4); \end{aligned} \quad (2.28)$$

$$F_{(i,j) \in \{-, -; +\}}^{[1,0]} = \eta_{i,j,3} (\Pi_1 - \Pi_2) (\Pi_3 - \Pi_4). \quad (2.29)$$

The perturbative limit (2.9) fixes the coefficients $\eta_{i,j,0}$ of (2.28) as

$$\eta_{i,j,0} = 3\delta_{i,D} \delta_{j,-} + \delta_{i,E} [\delta_{j,+} - (D-1)\delta_{j,0}]. \quad (2.30)$$

This representation then starts with a total of $8 \times 5 + 7 \times 1 = 47$ real, dimensionless coefficients. With no further restrictions on the latter, it would be adequate for quantities having partial Bose symmetry with respect to one distinguished channel, such as a two-particle irreducible kernel. For the full V_{4V} amplitude, imposing complete Bose symmetry by requiring equality with the two crossed forms produces 30 relations between the η 's so they can ultimately be expressed linearly in terms of the 17 independent ζ 's of (2.20). The listing of these linear conversion equations is relegated to Appendix B.2.

The r.h.s. of a DS equation such as Fig. 2 or Fig. 10 below, which singles out the leftmost external leg in an unsymmetric way, does not even exhibit the reduced symmetry of (2.28/2.29) (although it does have a permutation symmetry between the three rightmost legs). Upon using

(2.28/2.29) as input, the output therefore has still lower symmetry, and enforcing the self-consistency of a symmetric vertex turns out to imply, in addition to 47 self-reproduction conditions for the η 's, 7 more conditions for the vanishing of output terms violating the partial Bose symmetry, leading, after conversion of η 's to ζ 's, to a total of 54 linear conditions on the 17 independent coefficients. Moreover, one finds that unwanted contributions to the eight constants (2.30) arise which represent low- r approximation errors in the perturbative renormalization constant, a phenomenon already encountered in [2] for the three-point vertices.

Finally note that with respect to any one of the four p_i^2 , the reduced vertex permits a partial-fraction (p.f.) decomposition, such as

$$V_{4T}^{[r,0]} = E_{0,T}^{[r]}(p_2^2, p_3^2, p_4^2) + \sum_{n=1}^r \left(\frac{\Lambda^2}{p_1^2 + u_{2n}'' \Lambda^2} \right) E_{n,T}^{[r]}(p_2^2, p_3^2, p_4^2), \quad (2.31)$$

where by omitting p_1^2 dependence in the E_0 term we have encoded the restriction of no net positive powers of p_1^2 . Such a decomposition is useful technically in connection with the treatment of the compensating poles.

3 Self-consistency of compensating poles

It was demonstrated in [2] that from the lower (i.e., Γ_{3V} and Γ_{2V}) equations alone one may already infer the existence, and determine the residues, of certain pole terms in Γ_{4V} with respect to the three Mandelstam variables, and that these turn out (as did similar poles in longitudinal channels in the work of [4]) to be compensating terms cancelling unphysical singularities (“shadow” poles) in the one-gluon reducible terms of T_{4V} . The compensating poles are structures of tree topology which, since their internal shadow lines are not propagators of any of the elementary QCD fields, nevertheless can be present in the 1PI amplitude. This result is recalled in (1.1) and in Fig. 1(a), where each double-wiggly line, at level $[r, 0]$, stands for a set of r shadow poles in the corresponding Mandelstam variable.

To understand the nature of these structures more fully, we now need to discuss how they reproduce self-consistently in the DS equation for Γ_{4V} itself. As with all zeroth-order nonperturbative terms, this will essentially occur through the hierarchical DS coupling, which transfers the building materials for the compensating terms down from the higher vertices in the equation. The argument is lengthy, but conveys an idea of how, by analogy, such terms establish themselves in still higher vertex functions. We therefore present it also *in lieu of* a general N-legs-amplitudes proof, whose length would be out of proportion to the insight gained. (The reader not interested in the details of this self-consistency result, and willing to accept it on faith, may proceed directly to the reduced DS equation for V_{4V} given diagrammatically in Fig. 10, which is the starting point for Sect. 4.)

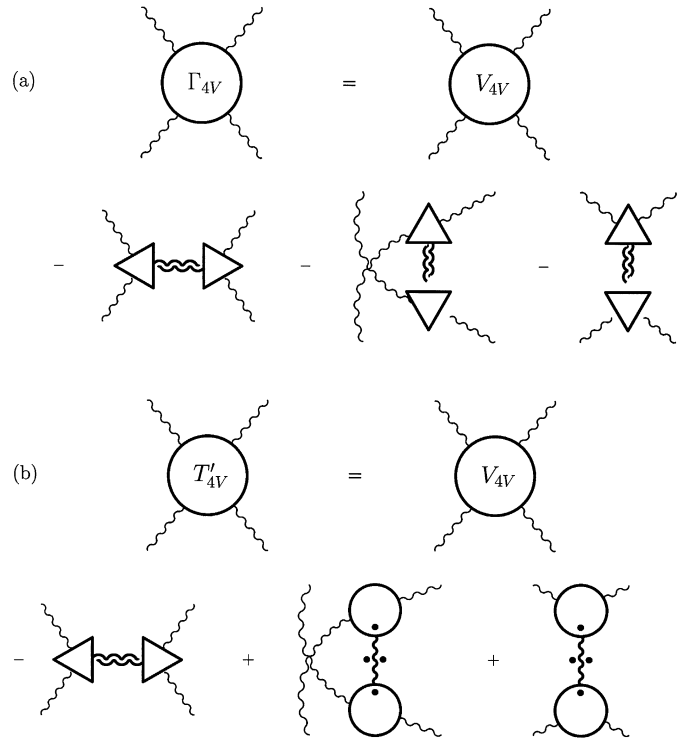


Fig. 1. a,b (a) Decomposition of 4-gluon vertex into reduced vertex and negative-shadow (“compensating”) poles. (b) Decomposition of partially irreducible 4-gluon amplitude T' into reduced vertex, compensating pole, and softened 1-gluon exchanges

(1) The equation for Γ_{4V} is written diagrammatically in Fig. 2, in a “hybrid” form in which interaction terms on the r.h.s. have not been resolved down to the level of proper vertices: the T' amplitudes appearing there are amputated functions 1PI in the channels defined by their right-hand external legs, but otherwise still contain 1PR terms. (A statement of a Γ_{4V} equation for the pure Yang-Mills case, and in a Bethe-Salpeter rather than DS form, may be found in [5]). The equation is derived by the standard procedure of starting from the “gluonic” equation of motion for the generating functional of covariantly quantized QCD (the functional derivative in this equation defines the distinguished, left-hand external leg in all terms of Fig. 2), performing three further functional differentiations with respect to the gluon field, putting all sources to zero, and transforming the resulting equation to the connected and finally to the 1PI function. In this process the terms denoted by $(C)_4, (C')_4, (C'')_4$, arise from the hierarchical coupling to the full six-gluon correlation function G_{6V} ; the latter has disconnected pieces of type $D \otimes G_{4V}$ which can contribute to the connected and the 1PI 4V-function equations, whereas the also existing disconnected G_{6V} pieces of type $G_{3V} \otimes G_{3V}$ are found to give only disconnected or 1PR terms for the 4V equation.

To keep technical complications to a minimum, we invoke all available simplifications: we disregard fermions, i.e. the term $(E)_4$ of Fig. 2, and consider zeroth-order self-consistency only at one loop, where term $(D)_4$ does not

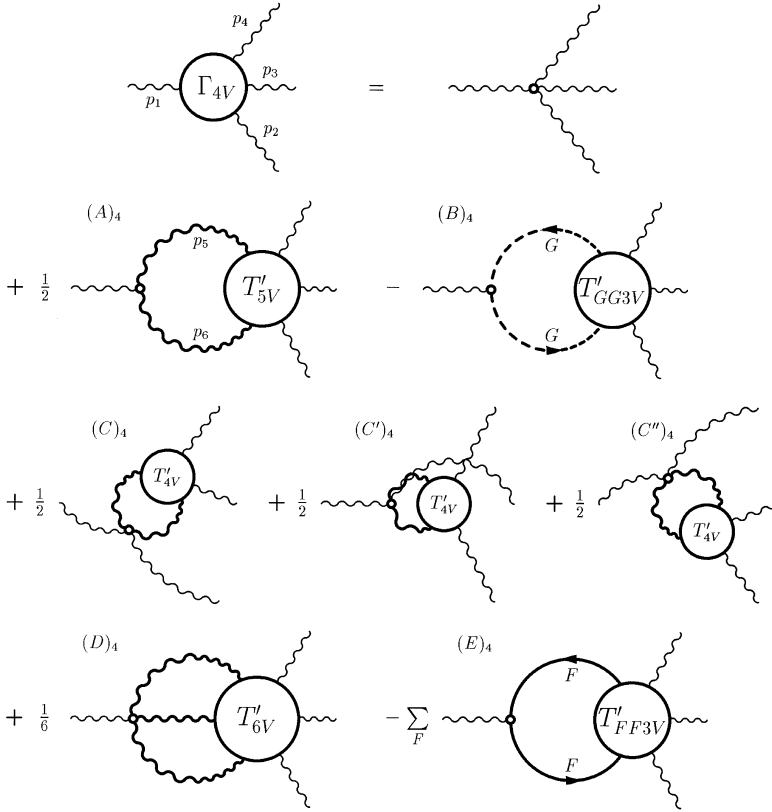


Fig. 2. DS equation for proper 4-gluon vertex in compact form, featuring partially irreducible T matrices

yet contribute, and in Landau gauge, so that the ghost term $(B)_4$ may also be omitted. (In principle, $(B)_4$ can contribute to the pole structures we are interested in, but the ghost propagator and ghost vertex from which the superficially convergent T_{GG3V} amplitude must be constructed remain perturbative in Landau gauge at one loop, as discussed in [2]. In this situation the amplitude therefore has no shadow terms, and the one-loop contributions to $(B)_4$ it produces remain equal to the perturbative graphs and bring only the perturbative divergences). We are then dealing, first, with terms $(C)_4, (C')_4, (C'')_4$, involving the four-gluon function itself in the form of three T'_{4V} amplitudes, each one-gluon irreducible in the channel defined by its two right-hand external legs. The structure of such a T'_{4V} as following from Fig. 1(a) is recalled in Fig. 1(b): it has one compensating (negative shadow) pole in the distinguished channel, and “softened” (one-shadow irreducible) one-gluon exchanges in the two other channels.

(2) Second, we have term $(A)_4$ involving a five-gluon amplitude T'_{5V} , which by definition is one-gluon irreducible in the four $2V \leftrightarrow 3V$ channels accessible through its three right-hand external legs, namely the “horizontal” channel

$$(5, 6) \leftrightarrow (2, 3, 4) \quad (i = 1), \quad (3.1)$$

and the three “tilted” channels

$$\begin{aligned} (2, 3) &\leftrightarrow (4, 5, 6) (i = 2), & (3, 4) &\leftrightarrow (5, 6, 2) (i = 3), \\ (4, 2) &\leftrightarrow (3, 5, 6) (i = 4). \end{aligned} \quad (3.2)$$

The integers i assigned refer, by convention, to a numbering $i = 1 \dots 10$ of the ten $2V \leftrightarrow 3V$ channels of a five-point amplitude. Thus T'_{5V} has those one-gluon reducible terms removed that would produce a one-gluon reducible graph when introduced into term $(A)_4$. A representation of T'_{5V} suitable for our purpose is given diagrammatically in Fig. 3; it is again hybrid in that it involves T'_{4V} amplitudes in addition to fully 1-gluon irreducible functions I_{4V} and I_{5V} . The derivation of this representation is a technical matter that we relegate to Appendix C. (Its apparent asymmetry with respect to the (5, 6) pair of legs is resolved by realizing that there exists an equivalent representation with the roles of I_{4V} and I_{4V} interchanged).

Insertion of Fig. 3 into the $(A)_4$ term of Fig. 2 then decomposes that term into a piece $(A)_{4,R}$ involving the 1-gluon irreducible I_{5V} , plus six pieces with triangle-graph topology. We do not draw this decomposition separately. (In non-Landau gauges there would be, in addition, a ghost term $-(B)_{4,R}$ involving a $\Gamma_{G\bar{G}3V}$ vertex, minus six ghost terms with box-graph topology, but as already stated we do not further discuss such gauges for simplicity).

(3) Now take residues in the Γ_{4V} equation of Fig. 2 with respect to the squared momentum, p_1^2 , of the left-most external leg. This is entirely analogous to the residue comparison performed in [2] for the Γ_{3V} equation, and leads to the analogous conclusion: the zeroth-order pole terms in p_1^2 of the r.h.s. can arise only from the term $(A)_{4,R}$, and the I_{5V} in that term must therefore contain

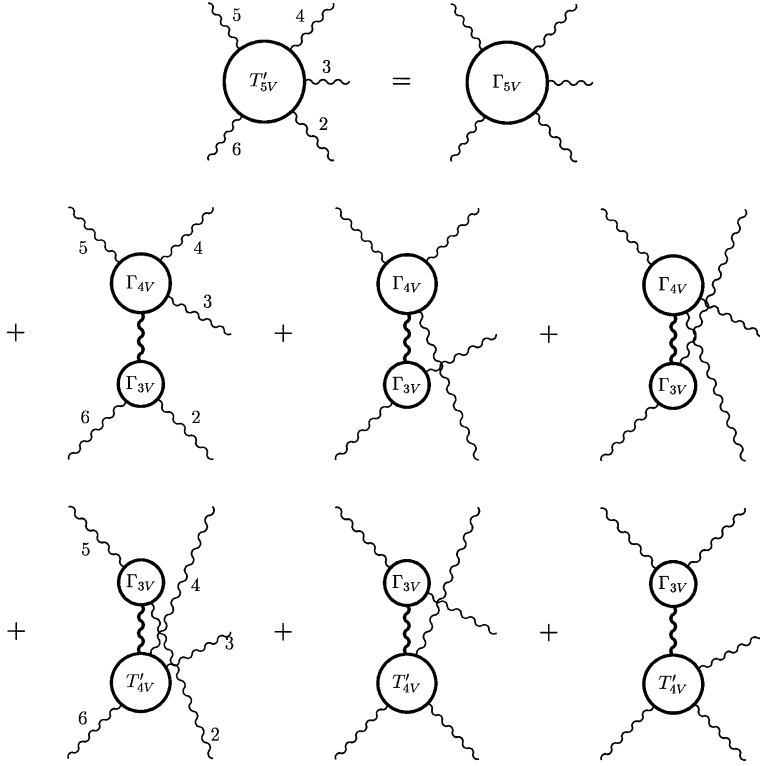


Fig. 3. Representation of partially 1-gluon-irreducible 5-gluon T matrix T'_{5V} . Γ_{5V} denotes the proper 5-gluon vertex. An equivalent representation has the roles of Γ_{4V} and T'_{4V} interchanged

zeroth-order poles $(s_1 + u_{2n}\Lambda^2)^{-1}$ (anticipating $u''_{2n} = u_{2n}$) in the Mandelstam variable of channel (3.1),

$$s_1 = (-p_5 - p_6)^2 = (p_2 + p_3 + p_4)^2, \quad (3.3)$$

which equals p_1^2 by momentum conservation. Note that terms with an inverse polynomial in p_1^2 produced by the *loop integration* of term $(A)_{4,\Gamma}$, if any, would by the standard formulas of dimensional integration have to arise from *convergent* parts of the integral, and therefore would not trigger the self-consistency mechanism for zeroth-order terms; they would be part of the *first-order*, quasi-perturbative correction - a remark indeed applying to all instances of generation of zeroth-order terms.

The residues of Γ_{5V} at those poles must be proportional to the residue functions $\mathcal{E}_n^{[r]}(p_2, p_3, p_4)$ ($1 \leq n \leq r$) in the p.f. decomposition of $\Gamma_{4V}^{[r,0]}$ analogous to (2.31). On the other side they must be proportional to the residue functions $B_n^{[r]}(p_5, p_6)$ ($1 \leq n \leq r$) of the three-point vertex Γ_{3V} ; this follows e.g. from the way the same Γ_{5V} amplitude enters in the two-DS-loops term of the three-point equation (term $(D)_3$ in Fig. 1 of [2]). For these pole terms of Γ_{5V} , the loop of $(A)_{4,\Gamma}$ then turns into loops of self-energy type already encountered in the self-consistency problem of $\Gamma_{2V}^{[r,0]}$, which fixes the proportionality factors: the internal lines in the zeroth-order pole terms of Γ_{5V} with respect to s_1 are associated with factors

$$-S_n^{[r]}(p_1) = -\frac{1}{u_{r,2n+1}} \frac{t(p_1)}{p_1^2 + u_{r,2n}\Lambda^2} \quad (n = 1 \dots r), \quad (3.4)$$

and therefore constitute minus a shadow line as defined in Fig. 3(b) of [2].

(4) To demonstrate self-consistency of the three negative-shadow terms in (1.1), we now feed the decomposition of Fig. 1(a) into the various contributing terms on the r.h.s. of Fig. 2 and verify that, upon appeal to information from the “lower” DS equations, those terms cooperate so that their sum splits off explicitly the same triplet of negative-shadow terms; after cancelling them from both sides of the equation, the remainder then constitutes a DS equation for the reduced amplitude V_{4V} .

The first place to feed in Fig. 1(a) is the Γ_{5V} poles just identified, with their $\mathcal{E}_n^{[r]}$ residue functions. This turns each of them into a pole with the corresponding reduced $E_n^{[r]}$ instead, minus a triplet of terms with *two* shadow poles each, involving in addition to the $B_n^{[r]}$ ($n \geq 1$) a set of functions $B_{m,n}^{[r]}$ defined by further decomposition of these,

$$B_m^{[r]}(p, q) = B_{m,0}^{[r]}(q) + \sum_{n=1}^r \left(\frac{\Lambda^2}{p^2 + u_{r,2n}\Lambda^2} \right) B_{m,n}^{[r]}(q) \quad (3.5)$$

Invoking now the full Bose symmetry of Γ_{5V} , we see that this vertex has a shadow-poles structure given, in a condensed notation, by

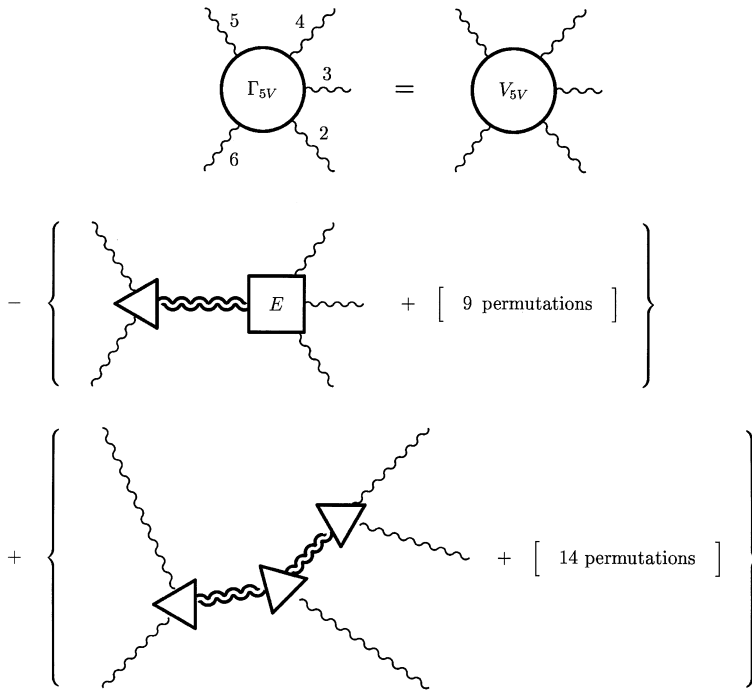


Fig. 4. Decomposition of proper 5-gluon vertex into reduced (1-gluon- and 1-shadow-irreducible) vertex V_{5V} , negative one-shadow terms in the 10 channels, and positive two-shadows terms for the 15 (2+1+2) partitions of the external legs

$$\begin{aligned}
 \Gamma_{5V} = & V_{5V} \\
 & - \sum_{i=1}^{10} \left\{ \sum_n B_n^{[r]} S_n^{[r]} E_n^{[r]} \right\}_i \\
 & + \sum_{k=1}^{15} \left\{ \sum_{m,n} B_m^{[r]} S_m^{[r]} B_{m,n}^{[r]} S_n^{[r]} B_n^{[r]} \right\}_k,
 \end{aligned} \tag{3.6}$$

where i enumerates the 10 channels, while k enumerates the 15 different 2+1+2 partitions of the 5 legs. This structure is shown diagrammatically in Fig. 4. Note that the symmetrization is achieved with only 15, not 30, of the latter terms: since each of them has shadow lines in two different channels, these are enough to supply the triplet of contributions mentioned before to pole structure in all of the 10 Mandelstam variables. The amplitude V_{5V} defined by (3.6) will be referred to as the reduced 5-gluon vertex. As a superficially convergent vertex with all tree-like structures removed by construction, it consists only of superficially convergent loops. Since these, as emphasized repeatedly, do not support the self-reproduction of zeroth-order terms, it is an exact statement that

$$V_{5V}^{[r,0]} = 0 \quad (\text{all } r). \tag{3.7}$$

(5) The next place to feed in the assertion of Fig. 1(a), or its consequence of Fig. 1(b), is the six terms of triangle topology, arising from $(A)_4$ of Fig. 2 upon insertion of the 1-gluon-reducible terms in the 2nd and 3rd lines of Fig. 3. Together with (3.6) and after some regrouping of terms, this is equivalent to using a new representation of the T'_{5V} amplitude given diagrammatically in Fig. 5. We again relegate details of its derivation to Appendix C and note only that this representation, apart from the fully one-shadow-irreducible gluon-exchange graphs in its 2nd

line, has a shadow-line content isolated in four terms: the negative-shadow term in the first line, which is identical to the $i = 1$ term in the 2nd line of (3.6) and will play a special role by supplying in Fig. 2 the singularities of V_{4V} in its p_1^2 variable, and the 3 negative terms in the last two lines, which involve a 3-gluon-1-shadow auxiliary amplitude Ξ_n as defined in Fig. 7.

(6) Lastly, we should introduce Fig. 1(b) into the $(C)_4$, $(C')_4$, and $(C'')_4$ terms of Fig. 2. This will turn each of them into a graph having a V_{4V} instead of T'_{4V} , plus a pair of one-shadow-irreducible gluon-exchange terms giving equal contributions and for which the factor of $\frac{1}{2}$ therefore gets cancelled, plus a negative term with one shadow line, as displayed in Fig. 8. (Note that an ordinary gluon line connecting to at least one *bare* vertex, such as the $\Gamma_{4V}^{(0)pert}$ in Fig. 8, has no shadow content).

(7) In the crucial step of the argument, we now refer back to the *three-point* vertex equation, maintaining for consistency the simplifications analogous to those of step (1) above, and again feed the assertion of Fig. 1 into the T'_{4V} term of that equation (term $(A)_3$ in Fig. 1 of [2]). We then take residues with respect to the squared momentum of one of the two external legs *other than* the “distinguished” leg entering from the left (one of the variables p_1^2 or p_3^2 in Fig. 1 of [2]). Note that this kind of residue information stood unused so far, since in [2] we only exploited residue comparison with respect to the distinguished leg. The result is the diagrammatic relation of Fig. 9, a DS equation of sorts for the partial amplitudes B_n ($n \geq 1$) of Γ_{3V} . (If we do not invoke the simplifications, this relation of course gets additional ghost-loop, fermion-loop, and two-gluon-loops terms with their own Ξ -type amplitudes, as alluded to in the last line of Fig. 9).

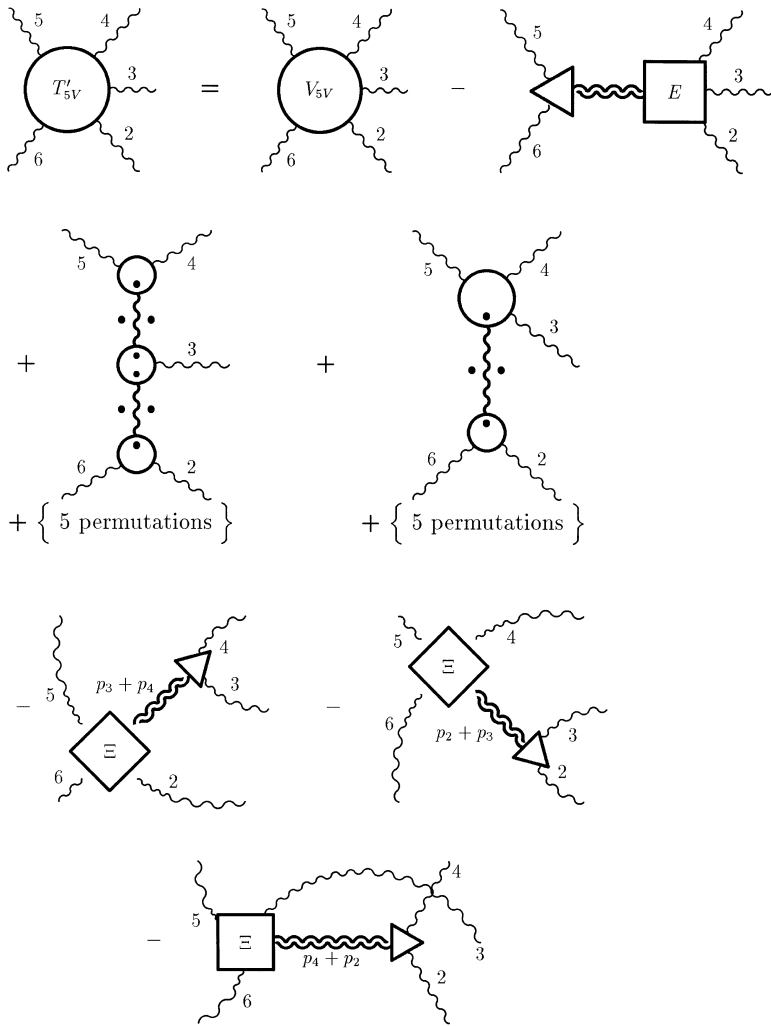


Fig. 5. Another representation of the T'_{5V} amplitude. The Ξ amplitudes in the last two lines are defined by Fig. 7

But this relation is precisely what is needed to turn the 3 negative shadow-line terms which arose in step (6) from the $(C)_4$ through $(C'')_4$ terms of Fig. 2, plus the 3 negative Ξ terms that arose from term $(A)_4$ upon insertion of the Ξ graphs of Fig. 5, into the 3 negative one-shadow terms on the r.h.s. of Fig. 1(a). We have therefore attained our goal: we have shown that upon introducing the decomposition of Fig. 1(a) with its 3 compensating-pole terms, either directly or through its immediate consequence of Fig. 1(b), into wherever a four-point building block occurs in the interaction terms of Fig. 2, these interaction terms cooperate so that their sum splits off explicitly those 3 compensating terms again. Note that in so doing we appealed to residue information not only from the lower (3-point and 2-point) DS equations, but now also from the 4-point equation itself, which led us to infer the shadow-reducibility structure (3.6) of the next higher, 5-gluon vertex.

We may now cancel the 3 compensating terms on both sides of the T_{4V} equation and thus establish the DS equation of Fig. 10 for the reduced vertex V_{4V} , which is the main result of this section.

(8) As a by-product, we may rewrite (3.6) for the shadow content of T_{5V} . To each of the 10 terms with nega-

tive signs in the second line, we may add a triplet of terms of structure $\sum_m T_{3V} D B_m S_m B_m$, with one ordinary-gluon and one shadow line, such that the resulting quartet of terms form precisely the set of compensating poles needed to cancel the four shadow lines present in the one-gluon-exchange diagram $\{T_{3V} D T_{4V}\}_i$ of the full connected-and-amputated 5-gluon amplitude T_{5V} (one along the D propagator line, the other three hidden, by Fig. 1(a), in the T_{4V} vertex). The same 30 terms, now regrouped into 15 suitable pairs, may then be subtracted from the 15 terms in the third line of (3.6), and it is straightforward to check with the aid of Fig. 6(b) that each resulting triplet then forms the set of compensating poles needed to cancel the one two-shadows term and two single-shadow terms present in a double-gluon-exchange diagram $\{T_{3V} D T_{3V} D T_{3V}\}_k$ of T_{5V} . Since the total operation has not changed the equation, we conclude, with a view to (C.1) of the Appendix, that

$$T_{5V} = V_{5V} + [\text{complete set of compensating poles for all 25 one-gluon-reducible terms of } T_{5V}]. \quad (3.8)$$

Thus the final result for the next higher amplitude is again simple: the full T_{5V} is completely one-shadow irreducible,

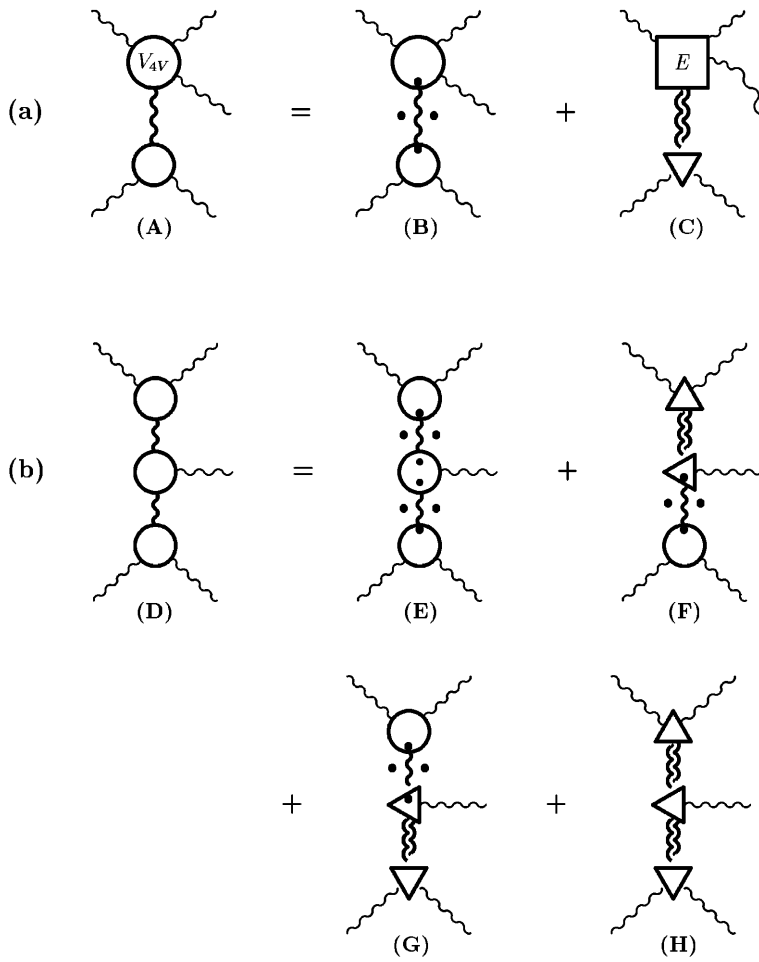


Fig. 6. Definition of (a) single and (b) double 1-shadow-irreducible (“softened”) gluon exchanges, marked by dots, through extraction of shadow terms from ordinary single and double gluon exchanges

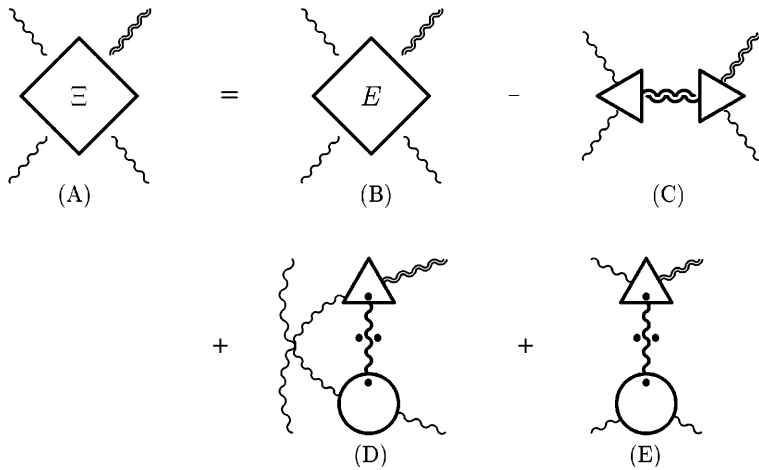


Fig. 7. Definition of 3-gluon-1-shadow auxiliary amplitudes Ξ

consisting as it does of a V_{5V} with full extended irreducibility, plus 25 “softened” (i.e. one-shadow irreducible) but still one-gluon reducible diagrams.

(9) Finally note that term $(A1)_4$ of the reduced V_{4V} equation of Fig. 10, upon taking residues at its horizontal-channel shadow poles and invoking once again the $\Gamma_{2V}^{[r,0]}$ self-consistency conditions, instantly reproduces the $E_n^{[r]}$

terms with $n \geq 1$ of the p.f. decomposition (2.31). The remaining, further-reduced equation for the partial amplitude $E_0^{[r]}$ of (2.31) at $r = 1$ is what we shall work with in practice; it should be kept in mind that this equation still has a term comprising the regular-at-poles remainders of $(A1)_4$ of Fig. 10.

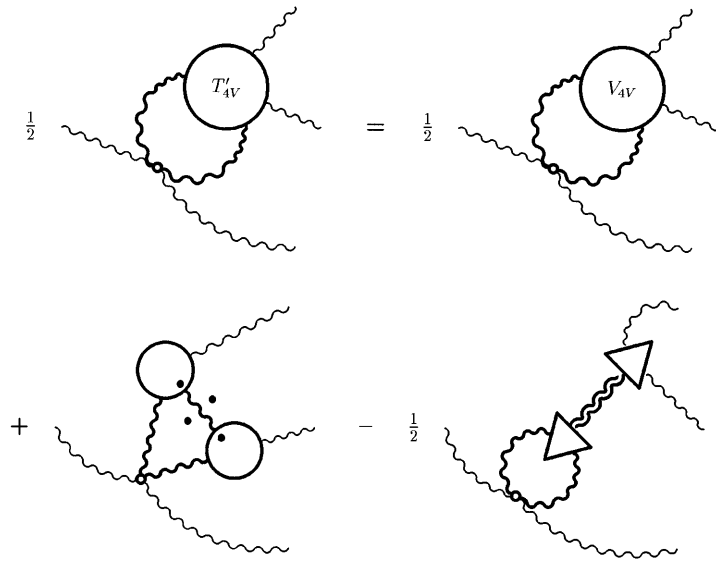


Fig. 8. Decomposition of the $(C)_4$ term of Fig. 2, obtained by use of Fig. 1(b)

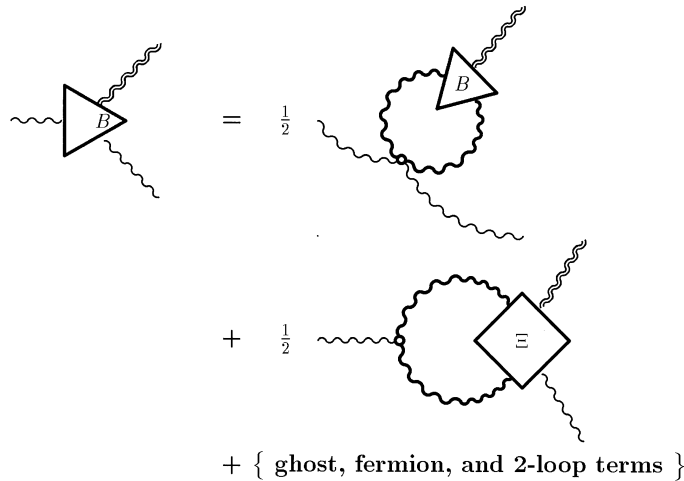


Fig. 9. DS-like integral equation for partial amplitudes B_n ($n \geq 1$) of 3-gluon vertex Γ_{3V} . The auxiliary amplitude Ξ in the second line is defined in Fig. 7

4 Self-consistency conditions

4.1 The overdetermined system

A glance at Fig. 10 shows that the reduced DS equation for V_{4T} , or for its $E_{0,T}$ component, is *linear* in the four-point unknowns, though still nonlinear in the “lower”, 2- and 3-point vertices. This simplification results from (i) the restriction to a one-loop calculation and (ii) our use of the ordinary DS system without Bethe-Salpeter resummation. The self-consistency equations for the ζ coefficients of (2.20) will thus form a linear system but with a matrix (determined by the divergent parts of diagrams $(A1)_4$, $(A3)_4$, and $(C2)_4$ of Fig. 10) and with inhomogeneous terms (determined by the divergent parts of the other diagrams of Fig. 10) depending nonlinearly on the 2-point and 3-point coefficients.

As discussed in [2], the zeroth-order self-consistency system as a whole exhibits a *scaling property*, arising from the scheme-insensitive character of the self-reproduction mechanism. It implies that the system only determines ratios of the nonperturbative coefficients to certain fixed powers of one of them. The latter, by convention, was chosen to be x_1 , a coefficient of the 3-transverse-gluons vertex. We need to maintain this convention for the 4-gluon quantities; thus for the parametrization (2.20) we introduce rescaled parameters

$$\tilde{\Lambda}^2 = |x_1| \Lambda^2, \quad \tilde{\zeta}_i = \zeta_i / |x_1|^{n_i} \quad (i = 1 \dots 17), \quad (4.1)$$

where the integers n_i are,

$$\begin{aligned} n_1 &= n_7 = n_{13} = 1, \\ n_2 &= n_3 = n_6 = n_8 = n_9 = n_{12} = n_{14} = n_{17} = 2, \\ n_4 &= n_{10} = n_{15} = 3, \\ n_5 &= n_{11} = n_{16} = 4. \end{aligned} \quad (4.2)$$

All RG-invariant masses are obtained in terms of $\tilde{\Lambda}^2$ rather than Λ^2 .

For the actual evaluation of the zeroth-order terms of diagrams $(A1)_4$, $(A3)_4$, $(C2)_4$ of Fig. 10, one uses parametrization (2.27) with its independent tensors and η coefficients. In contrast to what happens (at level $r = 1$) in the 3-point systems, the immediate self-reproduction of the entire p_1^2 -singular portion $E_{1,T}$ of (2.31), achieved by extracting the pole term at $p_1^2 = -u_2 \Lambda^2 = -\tilde{u}_2 \tilde{\Lambda}^2$ from diagrams $(A1)_4$ and appealing to the 2-gluon self-consistency conditions, is found not to provide substantial relief for the overdetermination caused by the lack of manifest Bose symmetry. After reimposing the symmetry by expressing all η 's in terms of the ζ coefficients of the fully Bose-symmetric form (2.20), one is still faced with 54 linear equations for these 17 basic coefficients, with matrix elements and inhomogeneities depending nonlinearly (though polynomially) on the lower-vertex coefficients. The complete system [3] is too lengthy to be

$$\begin{aligned}
 & - \left\{ \frac{1}{2} \right. \\
 & + (A2)_4 + \{ 2 \text{ permutations} \} \\
 & + (C1)_4 + \{ 2 \text{ permutations} \} \\
 & - \sum_F \{ 2 \text{ permutations} \} \\
 & - \{ \text{ghost terms not contributing to 0th order at } \xi = 0, l = 1 \} \\
 & + \{ \text{2-loop terms not contributing to 0th order at } l = 1 \} \\
 & + \{ V_3 \text{ terms not contributing to 0th order at any } r, l \}
 \end{aligned}$$

Fig. 10. DS equation for reduced 4-gluon vertex V_{4V} , obtained from Fig. 2 upon using Figs. 5, 8, and 9

listed here; we have therefore chosen to make it accessible through an electronic archive [8]. To convey an impression of its structure, we write here just one typical equation: self-reproduction of the coefficient $\eta_{A,0,4}$ in the invariant function (2.28) associated with the $C^{(A)} \otimes L_{(0)}$ tensor structure gives, after conversion to ζ 's by means of Appendix B.2 and multiplication by β_0 and u_3^2 , the condition

$$\begin{aligned}
 & \frac{9}{2} (u_3^2 x_3) \zeta_1 + \frac{9}{2} \left(\frac{3}{8} u_3^2 - u_3 x_4 \right) \zeta_2 \\
 & + \frac{3}{2} \left(\left(\frac{9}{8} - \beta_0 \right) u_3^2 - \frac{3}{2} u_3 x_4 \right) \zeta_3 \\
 & + \frac{27}{4} (u_3 x_1) \zeta_4 + \frac{9}{4} \left(\frac{3}{2} u_3^2 + u_3 x_4 \right) \zeta_6 \\
 & + \frac{3}{2} \left(\left(-\frac{9}{4} + \beta_0 \right) u_3^2 - \frac{3}{2} u_3 x_4 \right)
 \end{aligned}$$

$$\begin{aligned}
 & \times (\zeta_8 - 2\zeta_9 + 2\zeta_{12} - \zeta_{14} + \zeta_{17}) \\
 & + u_3 \left(\frac{99}{4} x_1 - \frac{15}{8} x_3 - N_F z_3 \right) (\zeta_{10} - \zeta_{15}) \\
 & = 9 \left(-\frac{3}{2} u_3^2 x_3^2 + 4u_3 x_1 x_3 x_4 + \left(\frac{1}{2} u_3 - x_2 \right) x_4^2 - 2x_1 x_4 x_5 \right) \\
 & + N_F \left(\frac{u_3}{w_3} \right)^2 \frac{2}{3} z_4 (w_3 z_1 z_3 - w_3 z_4 + z_1 z_5 - z_2 z_4). \quad (4.3)
 \end{aligned}$$

Here $N_C = 3$ has been used. The N_F factors identify contributions from the quark-loop diagrams $(E1)_4$, $(E1')_4$ and from the one in $(A1)_4$ of Fig. 10. Note that for the quark-vertex coefficients z_i , the simplified numbering of (4.6) of [2] has been employed.

As far as we are aware, no presently existing mathematical software tool for nonlinear algebraic systems is capable of dealing directly with a system of this size and complicated, partially overdetermined structure. The only

strategy currently practical for dealing with the total system is to take advantage of the “near decoupling” of the 4-point system: of the 17 ζ coefficients, only two combinations, Z_1 and Z_2 , enter the 2-and-3- point system (through some of the 3-gluon vertex conditions). One then treats these as additional unknowns in the lower-vertices system and, after invoking the scaling property, determines them to within an one-parameter freedom. Subsequently, their definitions are appended to the linear system for the 4-point ζ 's as two extra conditions, bringing the total to 56 equations: this represents only a minor increase in the anyway massive overdetermination of that system. The extra equations are, in rescaled form,

$$\frac{15}{32} (3\tilde{\zeta}_1 - \tilde{\zeta}_7) = \tilde{Z}_1 = \frac{Z_1}{x_1} \quad (4.4)$$

$$\frac{15}{32} (3\tilde{\zeta}_2 + 3\tilde{\zeta}_3 - \tilde{\zeta}_8 - \tilde{\zeta}_9) = \tilde{Z}_2 = \frac{Z_2}{x_1^2}, \quad (4.5)$$

where the \tilde{Z}_1, \tilde{Z}_2 on the r.h.s. stand for the values produced by the lower-vertices system. The structure of the four-point system then is,

$$\sum_{k=1}^{17} M_{ik}(\{\tilde{u}\}, \{\tilde{w}\}; \{\tilde{x}\}, \{\tilde{z}\}) \tilde{\zeta}_k = b_i(\{\tilde{u}\}, \{\tilde{w}\}; \{\tilde{x}\}, \{\tilde{z}\}) \quad (i = 1 \dots 56), \quad (4.6)$$

where the 56×17 matrix M , as well as the 56-component inhomogeneity b , depend nonlinearly on the rescaled coefficient sets $\{\tilde{u}\}, \{\tilde{w}\}$ of the gluon and quark two-point functions and on the sets $\{\tilde{x}\}, \{\tilde{z}\}$ of the gluon and quark three-point functions. Exceptions are the 55th and 56th rows of M , given by the l.h. sides of (4.4/4.5), which contain only pure numbers.

For a quasi-solution in the least-squares sense, one minimizes the quadratic deviation between both sides of (4.6). The conditions

$$\frac{\partial}{\partial \tilde{\zeta}_n} \left\{ \sum_{i=1}^{56} \left(\sum_k M_{ik} \tilde{\zeta}_k - b_i \right)^2 \right\} = 0 \quad (n = 1 \dots 17) \quad (4.7)$$

lead, in standard fashion, to a linear system with the 17×17 matrix $M^T M$,

$$\sum_{k=1}^{17} (M^T M)_{nk} \tilde{\zeta}_k = (M^T b)_n \quad (n = 1 \dots 17). \quad (4.8)$$

Although the structure of M is too complicated to be handled analytically, we have checked numerically that in the physically acceptable parameter range where all 2-and-3-point coefficients are real, the matrix $M^T M$ is always invertible. (The calculations have been performed using the MAPLE V computer-algebra system). As a measure of the deviation one may consider

$$\chi = \sqrt{\frac{1}{56} \sum_{i=1}^{56} \left(\sum_k M_{ik} \tilde{\zeta}_k - b_i \right)^2} \quad (4.9)$$

as compared to a typical r.h.s. or l.h.s. of (4.6). Also, the quantities \tilde{Z}_1, \tilde{Z}_2 when recalculated from the quasi-solution according to (4.4/4.5) will be different from their input values from the lower-vertices system, and the differences may serve as rough indicators of the overall degree of difficulty in satisfying zeroth-order self-consistency requirements from (ordinary) DS equations with the rather simple structure of the $r = 1$ set of approximants. If they are large, one may alternatively try to enforce conditions (4.4/4.5) exactly by assigning a large weight w (e.g. $w = 1000$) to the $i = 55$ and $i = 56$ terms of (4.7). The $Z_{1,2}$ from the two systems will then match, but the quality of the 54-term remainder solution will in general deteriorate.

4.2 Typical solution for $N_F = 2$

The entire system of course shares the effective one-parameter freedom from the “decoupled” lower-vertices system. In the presence of fermions, this was parametrized [2] by the coefficient \tilde{w}_1 . We only consider here the physically most interesting parameter range where not only all vertex coefficients are real, but also the values of the self-energy coefficients u, w imply the presence of a complex-conjugate pole pair in both the gluon and the fermion propagator. Over this range, as noted earlier, most of the other coefficients of the system do not vary substantially.

Table 1 gives least-squares values of the rescaled coefficients $\tilde{\zeta}$ corresponding to the “typical” solution of Table 1 of [2], which at $|w_1| = |w_2| = 0.6749$ (the signs of w_1, w_2 do not affect the 4-point system) is in about the middle of this parameter range. The two solutions shown are obtained either without extra weighting ($w = 1$) or with exact enforcement ($w = 1000$) of the 55th and 56th conditions. The resulting coefficients are generally rather large in absolute value, given the fact that from their very context one would expect them to be numbers of order unity (give or take an order of magnitude). This may partly be attributed to the choice of basis – the factors of $\frac{1}{4}, \frac{1}{6}, \frac{1}{12}$ in the tensors (2.18/2.19) employed in the W_n building blocks – and to the rescaling (4.1): it is conspicuous that the large coefficients mostly have large exponents n_i in (4.2). Although these effects may account for one to two orders of magnitude, several coefficients still remain implausibly large. We interpret this as the direct result of the considerable “pressure” generated by the overdetermination of the system.

The typical 2-and-3-point solution of [2] implies values of

$$\tilde{Z}_1 = 157.9, \quad \tilde{Z}_2 = 156.2 \quad (N_F = 2) \quad (4.10)$$

for the parameter combinations of (4.4/4.5) respectively. When not enforced (i.e. at $w = 1$), their values recalculated from the $\tilde{\zeta}$'s of Table 1, -335.95 and -165.07 , are strongly mismatched and even of the opposite sign. It is then hardly surprising to find that this solution has $\chi \approx 317$ in the sense of (4.9) – of the same magnitude as, or even slightly larger than, a typical $|b_i|$ in (4.6), which

Table 1. Coefficients $\tilde{\zeta}_n$ for $N_F = 2$ at typical value $\tilde{w}_1 = 0.67$

n	1	2	3	4	5	6	7	8	9
$\tilde{\zeta}_n(w = 10^3)$	56.22	646.67	-513.11	611.96	962.88	271.12	-168.19	-803.84	871.27
$\tilde{\zeta}_n(w = 1)$	-181.48	-98.04	-113.83	297.85	-2747.9	-37.55	172.27	-319.20	35.75
n	10	11	12	13	14	15	16	17	
$\tilde{\zeta}_n(w = 10^3)$	64.77	438.55	-202.04	-510.04	84.67	-561.86	-7481.9	209.80	
$\tilde{\zeta}_n(w = 1)$	1318.4	-1757.5	-26.14	76.28	190.68	367.79	5446.0	-317.7	

Table 2. Coefficients $\tilde{\zeta}_n$ for pure-gluon theory at typical value $\tilde{x}_3 = 1.0$

n	1	2	3	4	5	6	7	8	9
$\tilde{\zeta}_n(w = 10^3)$	0.814	6.439	-4.733	-57.35	350.05	-3.057	8.672	-30.03	0.931
$\tilde{\zeta}_n(w = 1)$	-0.432	9.285	-4.789	-54.834	255.08	-2.512	6.398	-21.50	1.275
n	10	11	12	13	14	15	16	17	
$\tilde{\zeta}_n(w = 10^3)$	96.02	-328.14	-0.060	3.354	-4.212	13.74	-121.67	-9.060	
$\tilde{\zeta}_n(w = 1)$	56.75	-110.07	-0.518	2.595	0.461	-19.15	124.0	-8.744	

is exemplified by (4.10) and of the order of a hundred. Enforcing the values (4.10) would then be expected to strongly alter the solution, which is indeed what happens – several of the coefficients even change signs, and χ deteriorates further to ≈ 349 . This is in marked contrast to the purely gluonic case discussed in the next subsection, and implies that in the presence of (massless) fermions the 4-point solution at the $r = 1$ level is probably a poor one. The presence of the massless-quark DS loops evidently makes the total system at low r much harder to satisfy; in particular these loops seem to work in the direction of forcing a mismatch at the (2+3)-point-to-4-point interface that can be alleviated only gradually at higher r .

4.3 Typical solution for pure-gluon theory

For pure Yang-Mills theory ($N_F = 0$) the typical solution, now parametrized by the gluonic coefficient \tilde{x}_3 as discussed in [2] and taken at $\tilde{x}_3 = 1$, leads to the 4-point $\tilde{\zeta}$'s given in Table 2.

Two features deserve comment. First, the coefficients overall are of a distinctly more plausible order of magnitude, entirely understandable from the above-discussed simple mechanisms; in particular, the three coefficients of sizes more than a hundred are precisely those with $n_i = 4$ in (4.2). Second, and more remarkably, the input $\tilde{Z}_{1,2}$ values from the lower-point system,

$$\tilde{Z}_1 = -2.92, \quad \tilde{Z}_2 = 16.04 \quad (N_F = 0) \quad (4.11)$$

are matched reasonably well by the four-point quasisolution even for $w = 1$, i.e. without being enforced exactly: when recalculated they come out as -3.60 and +15.80 respectively. Moreover, the χ value of ≈ 0.11 is now only about ten percent of the typical $|b_i|$ of (4.6), which in this case is of order unity. Exact enforcement of the values (4.11) then leads to no appreciable deterioration in χ .

This gives one confidence that *for the pure Yang-Mills system* the least-squares, four-point quasisolution does work reasonably well even on the $r = 1$ level of approximation – better, in fact, than one would expect in view of the still very simple and rigid structure of approximants at this level.

5 Conclusion

We have verified that self-consistent determination of a generalized Feynman rule for the highest superficially divergent and kinematically most complex QCD vertex is possible in principle, provided the overdetermination resulting from lack of manifest Bose symmetry in the relevant DS equation is dealt with by a least-squares procedure. Within the well-defined and clearly visible limitations of our calculation, available indicators suggest that the least-squares solution at level $r = 1$ is good for the pure gluon theory but quantitatively poor in the presence of massless quarks. For the Yang-Mills theory, the generalized Feynman-rule system determined in [2] and the present paper should be adequate, in spite of the low approximation order $r = 1$, as a basis for semi-quantitative calculations. For the system with massless quarks, in view of the large approximation errors found both here and in [2], the results do not yet seem sufficient to us for such applications; here we view our work as no more than a demonstration of technical feasibility of the self-consistency procedure as such.

Among the limitations, the one most obviously in need of improvement may be the use of an “ordinary” DS system: starting from BS-resummed dynamical equations (for amplitudes with three and more legs) would effectively shift more important physical effects into the lower loop orders, and would thereby give a one-loop self-consistency

calculation a better chance to succeed. It would also provide partial (though not complete) relief from the pressures of overdetermination: in BS-resummed equations the fraction of terms on the r.h.s. of a DS equation which are manifestly Bose symmetric individually, or can be grouped into manifestly symmetric subsets, is generally increased, so that one expects fewer symmetry-violating terms to be generated. Use of a tensor basis larger than our “dynamically minimal” one may not mitigate the overdetermination substantially, as it would also increase the number of self-consistency conditions, but would be necessary in order to allow d_{abc} color dependence in the three-gluon vertex to be treated consistently. Going beyond the $r = 1$ and $l = 1$ levels of approximation would have the algebraic complication rising steeply, as usual in iterative schemes for QFT, but is presumably the only consistent way of better satisfying perturbative limits and other desirable secondary conditions.

One possible strategy of improvement for the unsatisfactory situation with massless quarks may be to recall that a necessity (for self-consistency) of using approximants of the same order for all coupled vertex functions strictly speaking exists only within one type of external leg or elementary field. In particular it is possible, and would create no fundamental problems of consistency, to combine rational-approximation order $r = 3$ for fermionic legs (in the sense defined in Appendix (A.3/A.4) of [1], i.e. with respect to matrix-valued variables \not{p}) with the $r = 1$ approximation for bosonic legs as studied here. As the present study has shown, about ninety percent of the algebraic complication and computational effort for the total self-consistency system are caused by the four-gluon vertex alone; the fermion sector has no superficially divergent four-point or other amplitude of comparable difficulty. This type of improvement is therefore much more feasible than a full $r = 3$ calculation for all legs, and would seem to deserve priority in a further development of the method.

Appendix A Absence of non-compensating zeroth-order poles

Here we ask whether the four-gluon generalized Feynman rule $\Gamma_{4V}^{[r,0]}$ may contain, in addition to the “compensating” poles in its three crossed color-octet channels as identified in sect. 2.2 and made explicit in (1.1), still other poles of zeroth perturbative order in its Mandelstam variables. Such poles would be absent in the perturbative limit $\Lambda \rightarrow 0$, so their residue factors would be proportional to at least one power of Λ . In e.g. the s channel, such a pole would be of the form

$$\frac{\Lambda \Phi^T(p_1, p_2) \Lambda \Phi(p_3, p_4)}{P^2 + b\Lambda^2} \quad (\text{A.1})$$

with a dimensionless residue function (or vector of functions) Φ carrying the color and Lorentz quantum numbers of the channel considered. This contrasts with the case of the compensating pole, where residue comparison in

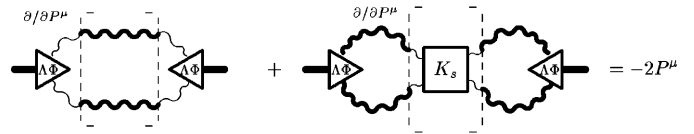


Fig. 11. Diagrammatic representation of Bethe-Salpeter normalization condition. The partial differentiations with respect to P_μ act on the portions in dashed brackets

the Γ_{3V} equation forces the residue factors to be proportional to B_n 's – quantities of mass dimension +1 which by themselves need not vanish as $\Lambda \rightarrow 0$ since in their defining equation ((2.15) of [2]) they are already accompanied by a Λ^2 factor.

The Bethe-Salpeter amplitudes $\Lambda\Phi$ must satisfy a well-known normalization condition [9], which in a condensed notation, and again in the most simplified form omitting ghost and fermion terms, reads

$$\begin{aligned} & \left\{ g_0^2 \frac{1}{2} \int \Lambda\Phi \left(\frac{\partial}{\partial P^\mu} (DD) \right) \Lambda\Phi \right\}_{P^2 = -b\Lambda^2} \\ & + \left\{ g_0^4 \frac{1}{4} \int \int \Lambda\Phi (DD) \left(\frac{\partial}{\partial P^\mu} K_s \right) (DD) \Lambda\Phi \right\}_{P^2 = -b\Lambda^2} \\ & = -2P^\mu. \end{aligned} \quad (\text{A.2})$$

This is depicted in Fig. 11. Fulfillment of this condition by purely zeroth-order quantities is possible only if the loop integrals on the l.h.s. diverge and thereby trigger the divergence-related $1/g^2$ mechanism. With the Φ functions behaving at worst like constants at large loop momenta q , and with the easily checked behavior of

$$\frac{\partial}{\partial P^\mu} (DD) = \mathcal{O}(q^{-5}), \quad \frac{\partial}{\partial P^\mu} K_s = \mathcal{O}(q^{-1}) \quad (\text{A.3})$$

(note that terms in K_s behaving like constants at large q 's, such as the $\Gamma^{(0)pert}$ term, drop out after differentiation), it is however clear that the integrals are convergent, and do not provide the $\frac{1}{\epsilon}$ factors necessary for the mechanism to work. Thus poles of type (A.1) in $T_{4V}^{[r,0]}$ are ruled out.

Note that the “compensating” poles, by contrast, *can* satisfy (A.2) as zeroth-order quantities, since there $\Lambda\Phi$ is replaced by a B_n (compare (2.22) of [2]) which at large q behaves like q^1 , and therefore provides divergences on the l.h.s. of (A.2).

Note also that if one does not insist on the Φ being quantities of zeroth perturbative order, (A.2) may be satisfied, at suitable eigenvalues $-b\Lambda^2$ of P^2 , by quantities which have no overall Λ factor but are power series starting at least at first order in g^2 . This, as emphasized in the introduction, is the case for ordinary bound-state poles, which arise from a Bethe-Salpeter partial resummation of the perturbation series for Γ_{4V} .

Appendix B Parametrizations of the reduced four-gluon vertex

Appendix B.1 Building blocks for the symmetric parametrization

To list the building blocks $W_n^{[1,0]}$ of the fully Bose-symmetric V_{4V} representation (2.20), we use the following combinations of single-pole quantities (2.13):

$$G_{(1)}(p_1^2 \dots p_4^2) = \Pi_1 + \Pi_2 + \Pi_3 + \Pi_4; \quad (\text{B.1})$$

$$G_{(2s)}(p_1^2 \dots p_4^2) = \Pi_1 \Pi_2 + \Pi_3 \Pi_4,$$

$$G_{(2u)}(p_1^2 \dots p_4^2) = \Pi_1 \Pi_3 + \Pi_4 \Pi_2,$$

$$G_{(2t)}(p_1^2 \dots p_4^2) = \Pi_1 \Pi_4 + \Pi_2 \Pi_3; \quad (\text{B.2})$$

$$G_{(3)}(p_1^2 \dots p_4^2) = \Pi_1 \Pi_2 \Pi_3 + \Pi_1 \Pi_2 \Pi_4 \\ + \Pi_1 \Pi_3 \Pi_4 + \Pi_2 \Pi_3 \Pi_4; \quad (\text{B.3})$$

$$G_{(4)}(p_1^2 \dots p_4^2) = \Pi_1 \Pi_2 \Pi_3 \Pi_4. \quad (\text{B.4})$$

Here $G_{(1)}$, $G_{(3)}$, and $G_{(4)}$ are Bose-symmetric in themselves, while G_{2s} , G_{2u} , and G_{2t} form a crossing triplet. In terms of these,

$$W_1^{[1,0]} := \left\{ C^{(S)} [L_{(3)} - 2L_{(1)} + L_{(2)}] \right. \\ \left. + (\text{perms. } s \rightarrow u, s \rightarrow t) \right\} G_{(1)}; \quad (\text{B.5})$$

$$W_2^{[1,0]} := \left\{ C^{(S)} [L_{(3)} - 2L_{(1)} + L_{(2)}] \right. \\ \left. + (\text{perms. } s \rightarrow u, s \rightarrow t) \right\} \\ \times (G_{(2s)} + G_{(2u)} + G_{(2t)}); \quad (\text{B.6})$$

$$W_3^{[1,0]} := \left\{ C^{(S)} [L_{(3)} - 2L_{(1)} + L_{(2)}] \right. \\ \left. \times [G_{(2t)} - 2G_{(2s)} + G_{(2u)}] \right\} \\ + (\text{perms. } s \rightarrow u, s \rightarrow t); \quad (\text{B.7})$$

$$W_4^{[1,0]} := \left\{ C^{(S)} [L_{(3)} - 2L_{(1)} + L_{(2)}] \right. \\ \left. + (\text{perms. } s \rightarrow u, s \rightarrow t) \right\} G_{(3)}; \quad (\text{B.8})$$

$$W_5^{[1,0]} := \left\{ C^{(S)} [L_{(3)} - 2L_{(1)} + L_{(2)}] \right. \\ \left. + (\text{perms. } s \rightarrow u, s \rightarrow t) \right\} G_{(4)}; \quad (\text{B.9})$$

$$W_6^{[1,0]} := \left\{ \frac{1}{4} C^{(1)} [L_{(1)} + L_{(2)} + L_{(3)}] \right. \\ \left. \times [G_{(2t)} - 2G_{(2s)} + G_{(2u)}] \right\} \\ + (\text{perms. } s \rightarrow u, s \rightarrow t); \quad (\text{B.10})$$

$$W_7^{[1,0]} := \left\{ \frac{1}{4} C^{(1)} [L_{(3)} - 2L_{(1)} + L_{(2)}] \right. \\ \left. + (\text{perms. } s \rightarrow u, s \rightarrow t) \right\} G_{(1)}; \quad (\text{B.11})$$

$$W_8^{[1,0]} := \left\{ \frac{1}{4} C^{(1)} [L_{(3)} - 2L_{(1)} + L_{(2)}] \right. \\ \left. + (\text{perms. } s \rightarrow u, s \rightarrow t) \right\} \\ \times (G_{(2s)} + G_{(2u)} + G_{(2t)}); \quad (\text{B.12})$$

$$W_9^{[1,0]} := \left\{ \frac{1}{4} C^{(1)} [L_{(3)} - 2L_{(1)} + L_{(2)}] \right. \\ \left. \times [G_{(2t)} - 2G_{(2s)} + G_{(2u)}] \right\} \\ + (\text{perms. } s \rightarrow u, s \rightarrow t); \quad (\text{B.13})$$

$$W_{10}^{[1,0]} := \left\{ \frac{1}{4} C^{(1)} [L_{(3)} - 2L_{(1)} + L_{(2)}] \right. \\ \left. + (\text{perms. } s \rightarrow u, s \rightarrow t) \right\} G_{(3)}; \quad (\text{B.14})$$

$$W_{11}^{[1,0]} := \left\{ \frac{1}{4} C^{(1)} [L_{(3)} - 2L_{(1)} + L_{(2)}] \right. \\ \left. + (\text{perms. } s \rightarrow u, s \rightarrow t) \right\} G_{(4)}; \quad (\text{B.15})$$

$$W_{12}^{[1,0]} := \left\{ \frac{1}{4} C^{(1)} [L_{(1)} + L_{(2)} + L_{(3)}] \right. \\ \left. \times [G_{(2t)} - 2G_{(2s)} + G_{(2u)}] \right\} \\ + (\text{perms. } s \rightarrow u, s \rightarrow t); \quad (\text{B.16})$$

$$W_{13}^{[1,0]} := \frac{1}{4} [C^{(1)} + C^{(2)} + C^{(3)}] \\ \times [L_{(1)} + L_{(2)} + L_{(3)}] G_{(1)}; \quad (\text{B.17})$$

$$W_{14}^{[1,0]} := \frac{1}{4} [C^{(1)} + C^{(2)} + C^{(3)}] [L_{(1)} + L_{(2)} + L_{(3)}] \\ \times [G_{(2t)} + G_{(2s)} + G_{(2u)}]; \quad (\text{B.18})$$

$$W_{15}^{[1,0]} := \frac{1}{4} [C^{(1)} + C^{(2)} + C^{(3)}] \\ \times [L_{(1)} + L_{(2)} + L_{(3)}] G_{(3)}; \quad (\text{B.19})$$

$$W_{16}^{[1,0]} := \frac{1}{4} [C^{(1)} + C^{(2)} + C^{(3)}] \\ \times [L_{(1)} + L_{(2)} + L_{(3)}] G_{(4)}; \quad (\text{B.20})$$

$$W_{17}^{[1,0]} := \frac{1}{4} [C^{(1)} + C^{(2)} + C^{(3)}] \\ \times \left\{ [L_{(3)} - 2L_{(1)} + L_{(2)}] G_{(2s)} \right. \\ \left. + (\text{perms. } s \rightarrow u, s \rightarrow t) \right\}. \quad (\text{B.21})$$

Appendix B.2 Relation between parametrizations

To obtain the expressions for the η parameters of (2.28) and (2.29) in terms of the 17 ζ coefficients, one rewrites the $W_n^{[1,0]}$ building blocks (as listed above) in (2.20) in terms of the linearly independent color tensors (2.22/2.23) and the s -channel-adapted Lorentz tensors (2.24/2.25) and compares coefficients with (2.27). The ensuing relations are,

$$\eta_{A,0,1} = -\frac{3}{2} \zeta_7 + \frac{3}{2} \zeta_{13} \quad (\text{B.22})$$

$$\begin{aligned}\eta_{A,0,2} &= -\frac{3}{4}\zeta_3 - \frac{3}{2}\zeta_8 - \frac{3}{2}\zeta_9 \\ &\quad + \frac{3}{2}\zeta_{12} + \frac{3}{2}\zeta_{14} + \frac{3}{4}\zeta_{17}\end{aligned}\quad (\text{B.23})$$

$$\begin{aligned}\eta_{A,0,4} &= \frac{3}{2}\zeta_3 - \frac{3}{2}\zeta_8 + 3\zeta_9 - 3\zeta_{12} \\ &\quad + \frac{3}{2}\zeta_{14} - \frac{3}{2}\zeta_{17}\end{aligned}\quad (\text{B.24})$$

$$\eta_{A,0,5} = -\frac{3}{2}\zeta_{10} + \frac{3}{2}\zeta_{15}\quad (\text{B.25})$$

$$\eta_{A,0,6} = -\frac{3}{2}\zeta_{11} + \frac{3}{2}\zeta_{16}\quad (\text{B.26})$$

$$\eta_{A,+1} = -\frac{1}{2}\zeta_7 + \frac{1}{2}\zeta_{13}\quad (\text{B.27})$$

$$\begin{aligned}\eta_{A,+2} &= \frac{1}{4}\zeta_3 + \frac{1}{2}\zeta_8 + \frac{1}{2}\zeta_9 \\ &\quad + \frac{1}{2}\zeta_{12} + \frac{1}{2}\zeta_{14} - \frac{1}{4}\zeta_{17}\end{aligned}\quad (\text{B.28})$$

$$\begin{aligned}\eta_{A,+4} &= -\frac{1}{2}\zeta_3 + \frac{1}{2}\zeta_8 - \zeta_9 - \zeta_{12} \\ &\quad + \frac{1}{2}\zeta_{14} + \frac{1}{2}\zeta_{17}\end{aligned}\quad (\text{B.29})$$

$$\eta_{A,+5} = \frac{1}{2}\zeta_{10} + \frac{1}{2}\zeta_{15}\quad (\text{B.30})$$

$$\eta_{A,+6} = \frac{1}{2}\zeta_{11} + \frac{1}{2}\zeta_{16}\quad (\text{B.31})$$

$$\eta_{A,-3} = \frac{3}{4}\zeta_3 - \frac{3}{4}\zeta_{17}\quad (\text{B.32})$$

$$\eta_{B,0,1} = \frac{3}{4}\zeta_7 + \frac{3}{2}\zeta_{13}\quad (\text{B.33})$$

$$\begin{aligned}\eta_{B,0,2} &= -\frac{3}{4}\zeta_3 + \frac{3}{4}\zeta_8 - \frac{3}{8}\zeta_9 \\ &\quad - \frac{3}{4}\zeta_{12} + \frac{3}{2}\zeta_{14} + \frac{3}{4}\zeta_{17}\end{aligned}\quad (\text{B.34})$$

$$\begin{aligned}\eta_{B,0,4} &= \frac{3}{2}\zeta_3 + \frac{3}{4}\zeta_8 + \frac{3}{4}\zeta_9 \\ &\quad + \frac{3}{2}\zeta_{12} + \frac{3}{2}\zeta_{14} - \frac{3}{2}\zeta_{17}\end{aligned}\quad (\text{B.35})$$

$$\eta_{B,0,5} = \frac{3}{4}\zeta_{10} + \frac{3}{2}\zeta_{15}\quad (\text{B.36})$$

$$\eta_{B,0,6} = \frac{3}{4}\zeta_{11} + \frac{3}{2}\zeta_{16}\quad (\text{B.37})$$

$$\eta_{B,+1} = -\frac{1}{4}\zeta_7 + \frac{1}{2}\zeta_{13}\quad (\text{B.38})$$

$$\begin{aligned}\eta_{B,+2} &= \frac{1}{4}\zeta_3 - \frac{1}{4}\zeta_8 + \frac{1}{8}\zeta_9 \\ &\quad - \frac{1}{4}\zeta_{12} + \frac{1}{2}\zeta_{14} - \frac{1}{4}\zeta_{17}\end{aligned}\quad (\text{B.39})$$

$$\begin{aligned}\eta_{B,+4} &= -\frac{1}{2}\zeta_3 - \frac{1}{4}\zeta_8 - \frac{1}{4}\zeta_9 \\ &\quad + \frac{1}{2}\zeta_{12} + \frac{1}{2}\zeta_{14} + \frac{1}{2}\zeta_{17}\end{aligned}\quad (\text{B.40})$$

$$\eta_{B,+5} = -\frac{1}{4}\zeta_{10} + \frac{1}{2}\zeta_{15}\quad (\text{B.41})$$

$$\eta_{B,+6} = -\frac{1}{4}\zeta_{11} + \frac{1}{2}\zeta_{16}\quad (\text{B.42})$$

$$\eta_{B,-3} = \frac{3}{4}\zeta_3 + \frac{9}{8}\zeta_9 - \frac{3}{4}\zeta_{17}\quad (\text{B.43})$$

$$\eta_{C,0,3} = -\frac{9}{8}\zeta_9 - \frac{9}{4}\zeta_{12}\quad (\text{B.44})$$

$$\eta_{C,+3} = \frac{3}{8}\zeta_9 - \frac{3}{4}\zeta_{12}\quad (\text{B.45})$$

$$\eta_{C,-1} = -\frac{3}{4}\zeta_7\quad (\text{B.46})$$

$$\eta_{C,-2} = -\frac{3}{4}\zeta_8 + \frac{3}{8}\zeta_9\quad (\text{B.47})$$

$$\eta_{C,-4} = -\frac{3}{4}\zeta_8 - \frac{3}{4}\zeta_9\quad (\text{B.48})$$

$$\eta_{C,-5} = -\frac{3}{4}\zeta_{10}\quad (\text{B.49})$$

$$\eta_{C,-6} = -\frac{3}{4}\zeta_{11}\quad (\text{B.50})$$

$$\eta_{D,0,3} = \frac{9}{4}\zeta_3 + \frac{9}{2}\zeta_6\quad (\text{B.51})$$

$$\eta_{D,+3} = -\frac{3}{4}\zeta_3 + \frac{3}{2}\zeta_6\quad (\text{B.52})$$

$$\eta_{D,-1} = \frac{3}{2}\zeta_1\quad (\text{B.53})$$

$$\eta_{D,-2} = \frac{3}{2}\zeta_2 - \frac{3}{4}\zeta_3\quad (\text{B.54})$$

$$\eta_{D,-4} = \frac{3}{2}\zeta_2 + \frac{3}{2}\zeta_3\quad (\text{B.55})$$

$$\eta_{D,-5} = \frac{3}{2}\zeta_4\quad (\text{B.56})$$

$$\eta_{D,-6} = \frac{3}{2}\zeta_5\quad (\text{B.57})$$

$$\eta_{E,0,1} = -\frac{3}{2}\zeta_1\quad (\text{B.58})$$

$$\eta_{E,0,2} = -\frac{3}{2}\zeta_2 - \frac{3}{4}\zeta_3 + \frac{3}{2}\zeta_6\quad (\text{B.59})$$

$$\eta_{E,0,4} = -\frac{3}{2}\zeta_2 + \frac{3}{2}\zeta_3 - 3\zeta_6\quad (\text{B.60})$$

$$\eta_{E,0,5} = -\frac{3}{2}\zeta_4\quad (\text{B.61})$$

$$\eta_{E,0,6} = -\frac{3}{2}\zeta_5\quad (\text{B.62})$$

$$\eta_{E,+1} = \frac{1}{2}\zeta_1\quad (\text{B.63})$$

$$\eta_{E,+2} = \frac{1}{2}\zeta_2 + \frac{1}{4}\zeta_3 + \frac{1}{2}\zeta_6\quad (\text{B.64})$$

$$\eta_{E,+4} = \frac{1}{2}\zeta_2 - \frac{1}{2}\zeta_3 - \zeta_6\quad (\text{B.65})$$

$$\eta_{E,+5} = \frac{1}{2}\zeta_4\quad (\text{B.66})$$

$$\eta_{E,+6} = \frac{1}{2}\zeta_5\quad (\text{B.67})$$

$$\eta_{E,-3} = -\frac{3}{4}\zeta_3.\quad (\text{B.68})$$

Appendix C Representations of the amplitude T'_{5V}

Here we sketch derivations for two different representations of the partially irreducible 5-gluon amplitude T'_{5V} needed in the argument of sect. 3.

(1) To establish the representation given in Fig. 3, start from the full connected and amputated 5-gluon amplitude (off-shell 5-gluon T matrix), T_{5V} . It has 25 one-gluon-reducible terms (dressed tree diagrams): one of structure $\Gamma_{3V} D \Gamma_{4V}$, reducible along a single internal gluon line, for each of the 10 different 2+3 partitions (or $2V \leftrightarrow 3V$ channels) of the 5 legs, and one of structure $\Gamma_{3V} D \Gamma_{3V} D \Gamma_{3V}$, reducible along two different internal lines, for each of the 15 different 2+1+2 partitions of the 5 legs. In the condensed notation adopted for (3.6), we have

$$T_{5V} = I_{5V} + \sum_{i=1}^{10} \{ \Gamma_{3V} D \Gamma_{4V} \}_i + \sum_{k=1}^{15} \{ \Gamma_{3V} D \Gamma_{3V} D \Gamma_{3V} \}_k. \quad (\text{C.1})$$

Of these one-gluon-reducible terms, 13 are reducible in at least one of the four channels (3.1/3.2), and therefore by definition are to be excluded from the T'_{5V} amplitude, leaving the latter to consist of the fully one-gluon-irreducible piece (proper vertex) I_{5V} , plus 12 dressed-tree diagrams still reducible in other channels – 6 from the second and 6 from the third line of (C.1).

The 6 one-gluon exchange terms from the second line of (C.1) are those in which one of the two legs no. 5 and 6 entering from the left in Fig. 3 connects to the Γ_{3V} , while the other connects to the Γ_{4V} . The 3 terms in which leg no. 6 connects to a Γ_{3V} constitute the second line of Fig. 3. The 3 terms in which leg no. 5 connects to the Γ_{3V} may each be taken together with a suitable pair from among the 6 terms retained of the third line of (C.1), in such a way as to replace their Γ_{4V} 's with T'_{4V} 's whose primes refer to the channels defined by their external-line pairs. (Remember that, by definition, $T'_{4V} = \Gamma_{4V}$ plus 2 one-gluon exchange terms in the channels other than the distinguished channel to which the prime refers). This establishes the third line of Fig. 3.

Of course, in this regrouping the roles of legs 5 and 6 may be interchanged, leading to a representation equivalent to Fig. 3 in which the T'_{4V} 's and Γ_{4V} 's have their roles exchanged. This explains the apparent asymmetry of Fig. 3.

(2) The representation of T'_{5V} given in Fig. 5 is established by (i) applying the decomposition of (3.6) to the I_{5V} in the first line of Fig. 3, (ii) inserting the decompositions of Fig. 1(a) and Fig. 1(b) into the Γ_{4V} and the T'_{4V} terms of Fig. 3 respectively, and (iii) performing

decompositions of the remaining ordinary gluon lines into “softened” one-gluon exchanges and shadow-pole terms as indicated in Fig. 6. (As for Fig. 6(b), it lumps together for simplicity two decompositions, corresponding to its first and second lines, that actually occur separately). The six last terms of Fig. 3 then give rise to:

(a) 6 softened one-gluon-exchange graphs of the type of term (B) of Fig. 6, shown in the second line of Fig. 5,

(b) 6 graphs with two softened one-gluon exchanges each, of the type of term (E) of Fig. 6, also shown in the second line of Fig. 5,

(c) 6 one-shadow-line graphs as in term (C) of Fig. 6, which cancel 6 of the 10 negative terms coming from the second line of the I_{5V} decomposition (3.6), leaving just those four of the 10 negative terms that possess a shadow line in one of the four channels (3.1/3.2),

(d) 12 graphs with two shadow lines each of the type of term (H) of Fig. 6 – 9 from the Γ_{4V} and 3 from the T'_{4V} terms – with minus signs, which cancel 12 of the 15 terms from the third line of (3.6), leaving just those three of the 15 terms that have one shadow in the “horizontal” channel (3.1) and the other in one of the three “tilted” channels (3.2),

(e) 18 graphs with one softened-gluon exchange and one shadow line each: 12 with minus signs from both the Γ_{4V} and T'_{4V} terms, and 6 with plus signs from the T'_{4V} terms alone, and which actually cancel 6 of the minus-sign graphs, leaving a net count of 6 terms with one softened-gluon and one shadow line and with minus signs.

Now the 6 terms surviving from (e), the 3 two-shadows terms surviving from (d), and 3 of the 4 one-shadow terms from (c) may be lumped together in three groups by defining the auxiliary amplitudes Ξ_n as in Fig. 7; they then give the three graphs in the last two lines of Fig. 5. The one remaining one-shadow graph with minus sign from (c) appears explicitly in the first line of Fig. 5, which is therefore fully established.

References

1. M. Stingl, Z. Physik **A353** (1996) 423; E-print archive: hep-th/9502157
2. L. Driesen et al., Extended iterative scheme for QCD: three-point vertices, preceding article in this volume; E-print archive: hep-th/9808152
3. L. Driesen, Dr.rer.nat. thesis, University of Muenster, Germany, 1997 (unpublished)
4. R. Jackiw and K. Johnson, Phys. Rev. **D8** (1973) 2386, J.M. Cornwall and R.E. Norton, Phys.Rev. **D8** (1973) 3338
5. M. Baker and C. Lee, Phys. Rev. **D15** (1977) 2201
6. L.M. Kaplan and M. Resnikoff, J.Math.Phys. **8** (1967) 2194
7. J. Ahlbach et al., Phys. Lett. **B275** (1992) 124
8. L. Driesen and M. Stingl, E-print archive: hep-th/9808155, Appendix D
9. D. Lurié, A.J. Macfarlane and Y. Takahashi, Phys.Rev. **B140** (1965) 1091